

**Universidad Nacional de Mar del Plata, Facultad
de Ingeniería**

Departamento de Ingeniería en Materiales

**“MATRICES ELECTROHILADAS HÍBRIDAS de
PCL/ZEINA PARA INGENIERIA DE TEJIDOS BLANDOS”**

Augusto Nicolas Covone

Directores

- Dr. Gustavo A. Abraham Prof.
- Dr. Aldo R. Boccaccini

Supervisor:

- Ing. Francesco Iorio

**Proyecto final para optar al grado de Ingeniería en
Materiales**

Mar del Plata, abril 2024

Contacto: Covoneaugusto@gmail.com



RINFI es desarrollado por la Biblioteca de la Facultad de Ingeniería de la Universidad Nacional de Mar del Plata.

Tiene como objetivo recopilar, organizar, gestionar, difundir y preservar documentos digitales en Ingeniería, Ciencia y Tecnología de Materiales y Ciencias Afines.

A través del Acceso Abierto, se pretende aumentar la visibilidad y el impacto de los resultados de la investigación, asumiendo las políticas y cumpliendo con los protocolos y estándares internacionales para la interoperabilidad entre repositorios



Esta obra está bajo una [Licencia Creative Commons Atribución- NoComercial-CompartirIgual 4.0 Internacional](https://creativecommons.org/licenses/by-nc-sa/4.0/).

**Universidad Nacional de Mar del Plata, Facultad
de Ingeniería**

Departamento de Ingeniería en Materiales

**“MATRICES ELECTROHILADAS HÍBRIDAS de
PCL/ZEINA PARA INGENIERIA DE TEJIDOS BLANDOS”**

Augusto Nicolas Covone

Directores

- Dr. Gustavo A. Abraham Prof.
- Dr. Aldo R. Boccaccini

Supervisor:

- Ing. Francesco Iorio

**Proyecto final para optar al grado de Ingeniería en
Materiales**

Mar del Plata, abril 2024

Contacto: Covoneaugusto@gmail.com



Resumen de Contenido:

Este proyecto presenta un estudio sobre la fabricación y caracterización de andamios basados en poli(ϵ -caprolactona) (PCL) y zeína / zeína entrecruzada preparados mediante la técnica de electrohilado verde. Se utilizó un sistema de solventes benignos (ácido acético/etanol). La zeína es una proteína vegetal ampliamente disponible, biodegradable y biocompatible con un creciente interés como vehículo para una amplia variedad de aplicaciones biomédicas. Sin embargo, su pobre rendimiento mecánico requiere la combinación con polímeros biocompatibles sintéticos para preparar andamios adecuados para aplicaciones de ingeniería de tejidos. El uso de solventes benignos o no tóxicos no es trivial ya que la mayoría de los solventes utilizados para el proceso de electrohilado son muy efectivos en la disolución de polímeros, proporcionando propiedades de solución deseables para el electrohilado, pero son altamente tóxicos tanto para el operador como para el medio ambiente. Además, las trazas residuales pueden comprometer la viabilidad celular.

Se exploraron diferentes proporciones de PCL-zeína/zeína entrecruzada. Los mejores parámetros de electrohilado se ajustaron a cada composición y solvente. Todas las fibras fueron caracterizadas y se utilizó la composición con las mejores propiedades para producir fibras electrohiladas alineadas para imitar la estructura nativa del tendón.

A través del análisis de estos ensayos, se obtuvieron resultados prometedores con mezclas de PCL/ZEINA en una proporción de 2:1. Se produjeron fibras alineadas que muestran características adecuadas para su uso en la ingeniería de tejidos tendinosos con estas mezclas.



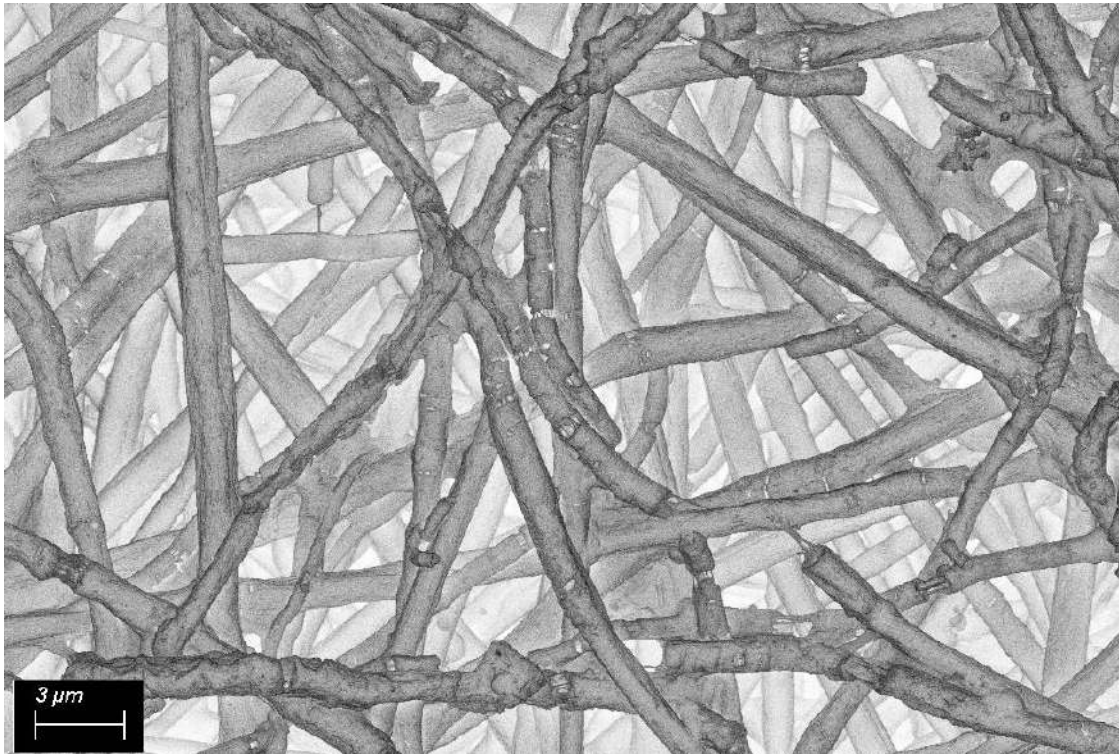
Facultad de Ingeniería, Universidad Nacional de Mar del Plata

Friedrich-Alexander Universität Erlangen-Nürnberg

Proyecto final de grado de Ingeniería en Materiales

**“MATRICES ELECTROHILADAS HÍBRIDAS de PCL/ZEINA
PARA INGENIERIA DE TEJIDOS BLANDOS”**

**“FABRICATION AND CHARACTERIZATION OF PCL-ZEIN
ELECTROSPUN FIBROUS SCAFFOLDS FOR TENDON TISSUE
ENGINEERING”**



AUGUSTO NICOLÁS COVONE

Directors:

Dr. Gustavo A. Abraham

Prof. Dr. Aldo R. Boccaccini

Supervisor: Francesco Iorio



RINFI se desarrolla en forma conjunta entre el INTEMA y la Biblioteca de la Facultad de Ingeniería de la Universidad Nacional de Mar del Plata.

Tiene como objetivo recopilar, organizar, gestionar, difundir y preservar documentos digitales en Ingeniería, Ciencia y Tecnología de Materiales y Ciencias Afines.

A través del Acceso Abierto, se pretende aumentar la visibilidad y el impacto de los resultados de la investigación, asumiendo las políticas y cumpliendo con los protocolos y estándares internacionales para la interoperabilidad entre repositorios



Esta obra está bajo una [Licencia Creative Commons](#)

[Atribución- NoComercial-CompartirIgual 4.0 Internacional.](#)

*agradecimientos

Index

1. Summary
2. Introduction
 - 2.1. Tendon
 - 2.1.1. Tendon structure
 - 2.1.2. Tendon wounds
 - 2.1.3. Tendon regeneration
 - 2.2. Tissue engineering of tendon
 - 2.2.1. Scaffold for tendon regeneration
 - 2.2.2. Materials for tendon tissue engineering
 - 2.2.3. Proteins
 - 2.2.4. Synthetic polymers
 - 2.3. Electrospinning technique
 - 2.3.1. Solution parameter
 - 2.3.1.1. Viscosity and concentration of polymer solutions
 - 2.3.1.2. Conductivity of solvents and polymers
 - 2.3.1.3. Polymer-solvent systems
 - 2.3.2. Processing parameters
 - 2.3.2.1. Flow rate
 - 2.3.2.2. Voltage
 - 2.3.2.3. Distance between needle and collector
3. Objectives
4. Materials
5. Methods
 - 5.1. Fabrication of electrospun scaffolds
 - 5.2. Microstructural and morphological characterization
 - 5.2.1. Scanning electron microscopy (SEM)
 - 5.2.2. Fourier transform infrared spectroscopy (FTIR)
 - 5.2.3. Mechanical tests
 - 5.2.4. Contact angle measurements
 - 5.3. Degradation tests
 - 5.4. Cell Tests
 - 5.4.1. Cell viability
 - 5.4.2. Cell adhesion
 - 5.4.3. ALP activity
6. Results and discussion
 - 6.1. Fabrication of electrospun scaffolds
 - 6.2. Microstructural and morphological characterization
 - 6.3. Degradation behavior
 - 6.4. Cell behaviour
7. Conclusions
8. References
9. Future works

List of Figures

- Figure 1:** Stress-strain curve for tendon. 9
- Figure 2:** Tendon structure from collagen molecules to the whole tendon. 10
- Figure 3:** Scheme of tissue engineering for tendon in vitro, starting from the autologous cells of the patient.13
- Figure 4:** Cartoon illustrations of structure models of zein according to Li et al. 18
- Figure 5:** Scheme of PCL chemical structure. 19
- Figure 6:** Electrospinning operating principle and Taylor cone formation.21
- Figure 7:** Different electrospinning collector: (a) flat plate collector; (b) drum collector rotating at low speed, producing random nanofibers; (c) drum collector rotating at high speed, producing aligned nanofibers. 21
- Figure 8:** Electrospinning equipment (Starter Kit 40KV Web) with a flat collector. Friedrich-Alexander-Universität Institute of Biomaterials (Erlangen, Germany).27
- Figure 9:** The influence of collectors on the final structure of the fibers. (a) typical random fibrous mat, (b) aligned fibers. 29
- Figure 10:** Plates for samples for SEM examination. 30
- Figure 11:**Set up of the mechanical test. 31
- Figure 12:** Fibrous mats with water drops during contact angle tests. 32
- Figure 13:** SEM images of the samples. (A) PCL/Zein 1:3 (B) PCL/Zein 3:4. 35
- Figure 14:** SEM images of the samples. (A) PCL 20%. (B) PCL/Zein 2:1 (Random). (C) PCL/Zein 1:1. (D) PCL/Zein 1:2. (E) PCL/Zein 2:1 (Aligned). 37
- Figure 15:** SEM micrographs of samples: (A) Zein AA. (B) Zein CC 1 h before spinning. (C) Zein CC 24 h before spinning. (D) Zein CC 72 h before spinning. 38
- Figure 16:** Histogram of the average fiber diameter. 39
- Figure 17:** Diameter distribution of all samples. 40
- Figure 18:** Diameter distribution of PCL/ZEIN 2:1 Aligned. 41
- Figure 19:** Direction of the fibers PCL/ZEIN 2:1 Random. 42
- Figure 20:** Direction of the fibers PCL/ZEIN 2:1 Aligned. 42
- Figure 21:** SEM micrograph of PCL/Zein 2:1 before (up) and after (down) degradation test. 43
- Figure 22:** SEM micrograph of PCL/Zein 2:1 after degradation for 7 (up), 14 (center) and 28 (down) days. 44
- Figure 23:** SEM micrograph of PCL/Zein 2:1 after 14 days of degradation..45
- Figure 24:** FTIR spectrum for ZEIN AA. 47
- Figure 25:** FTIR spectra for ZEIN CC at 1 h, 24 h and 72 h prep. before spinning.49
- Figure 26:** FTIR spectrum for PCL 20%. 50
- Figure 27:** FTIR spectra for PCL/ZEIN at 2:1, 1:1 and 1:2 ratios. 51
- Figure 28:** FTIR spectra for PCL/ZEIN 2:1 Aligned. 53
- Figure 29:** Difficulties in carrying out mechanical tests on Zein CC. 54
- Figure 30:** Zein AA samples after tensile tests. 55
- Figure 31:** Stress vs strain curves of Zein AA. 55
- Figure 32:** (A) PCL 20% Samples after tensile test. (B) Strain vs stress curve of PCL 20% Sample 1.56
- Figure 33:** PCL/ZEIN 2:1 samples after tensile test. 56
- Figure 34:** Stress vs Strain curves of PCL/ZEIN 2:1 Random. 57
- Figure 35:** PCL/ZEIN 1:1 samples after tensile test. 57
- Figure 36:** Image of PCL/ZEIN 1:1 sample showing delamination events. 58
- Figure 37:** Stress vs Strain curves of PCL/ZEIN 1:1. 58
- Figure 38:** PCL/ZEIN 1:2 samples after tensile tests. 59
- Figure 39:** Stress vs Strain curves PCL/ZEIN 1:2. 59
- Figure 40:** Stress vs strain curves PCL/ZEIN 2:1 with aligned nanofibers. 60
- Figure 41:** Water drops in contact angle measurements at 10 seconds for samples: (A) PCL 20%. (B) Zein 30%. 62

Figure 42: Water drops in contact angle measurements at 10 seconds for Zein CC samples: (A) 1 h, (B) 24 h, (C) 72 h. 63

Figure 43: Water drops in contact angle measurements at 10 seconds for PCL/ZEIN samples: (A) 2:1 , (B) 1:1 , (C) 1:2. 63

Figure 44: Water Uptake vs Incubation Time for PCL/ZEIN 2:1 Random. 64

Figure 45: Weight loss vs incubation time for PCL/ZEIN 2:1 (random). 65

Figure 46: Plate used for cell viability and ALP Activity. 66

Figure 47: Cell viability test. Left: After 7 days. Right: After 14 days. 67

Figure 48: WST-8 Results. 68

Figure 49: Zein CC 72 h sample. 69

Figure 50: PCL 20% Sample. 69

Figure 51: PCL/ ZEIN 2:1 random sample. 70

Figure 52: PCL/ZEIN 2:1 Aligned sample. 71

Figure 53: ALP activity vs incubation time. 72

List of Tables

Table 1: Parameters of electrospinning. 29

Table 2: Average fiber diameter and standard deviation of all samples. 39

Table 3: FTIR peaks for Zein AA. 49

Table 4: FTIR main bands assignment for Zein CC. 49

Table 5: FTIR main bands assignment for PCL 20%. 50

Table 6: FTIR main bands assignment for PCL/ZEIN blends. 52

Table 7: Tendency of the mechanical properties of all the samples. 61

Table 8:

List of Equations

Equation 1: Water Uptake (%). 32

Equation 2: Weight Loss (%). 32

Acknowledgments

Firstly, I would like to thank my supervisors Dr. Gustavo Abraham and Iorio Francesco for guiding and assisting me throughout my project.

Thanks to the IDEAR program for providing me with the opportunity to travel to Germany and carry out my final project. I would like to express my gratitude to Dra. Silvia Simison, Dr. Aldo Boccaccini, and Dr. Flavio Soldera for coordinating this project

Thanks to the professors and the Universidad Nacional de Mar del Plata for guiding me along this journey. Also, gratitude to Friedrich-Alexander-Universität Erlangen-Nürnberg for allowing me to conduct my final project at the Institute of Biomaterials.

Thanks to Rauschert Kloster Veilsdorf GmbH, for allowing me to carry out my professional practices in their facilities. Also thanks to Andreas, Hella, Frank, Slava and all my colleagues who made me feel at home even when I was away from my family and friends.

Thanks to Catalina, Luana and Ian for supporting me in Erlangen. Thanks to my family in Leon for receiving me at the time I needed it most. Thanks to Wojciech and Igor for opening the doors of their homes and taking me to see their country.

Finalmente quería agradecer a mis compañeros y amigos que me acompañaron incondicionalmente a través de estos años. A Gushi, Karim, Fede, Valentin, Lucas y todo aquel que me dio una mano cuando lo necesite. A mi familia, especialmente a hermana Giuliana y mis padres Natalia y Jorge por todo el cariño y paciencia que tuvieron conmigo. Por último, agradecer a Isabella por todo el amor y confianza que me permitieron atravesar todos los obstáculos. Sin ellos, nada de esto hubiese sido posible.

1. Summary

Scaffolds are supporting materials used in tissue engineering applications to repair or restore damaged tissues by providing a temporary or permanent three-dimensional framework for cells to grow, differentiate, and regenerate the damaged tissue. These scaffolds act as a structural support, guiding the formation of new tissue while promoting cell attachment, proliferation, and nutrient diffusion.

Scaffolds play a vital role in tissue engineering and regenerative medicine, facilitating the development of functional tissues and organs for transplantation or therapeutic purposes. Researchers tailor the properties of these scaffolds, including their porosity, mechanical strength, and degradation rate, to suit specific tissue types and the intended application. The use of stem cells on scaffolds allows driving cells to proliferate and regenerate tissues in specific directions. Biomaterials are often used to fabricate scaffolds composed of different types of biomaterials including biopolymers, synthetic polymers, bioceramics and biodegradable metals. The combination of synthetic and natural polymers can overcome some disadvantages of each one and produce new materials with superior properties.

Moreover, scaffolds can be combined with various biological factors like growth factors, cytokines, or even stem cells to enhance tissue regeneration further. By integrating these bioactive elements, scaffolds can stimulate specific cellular activities, modulate the tissue microenvironment, and promote more effective tissue healing and remodeling.

This project presents a study on the fabrication and characterization of polycaprolactone (PCL) and zein/crosslinked zein based scaffolds prepared by green electrospinning technique. A benign solvent system (acetic acid / ethanol) was used. Zein is a widely available, biodegradable, and biocompatible vegetal protein with rising interest as a carrier for a wide variety of biomedical applications. However, its poor mechanical performance requires the combination with synthetic biocompatible polymers to prepare suitable scaffolds for tissue engineering applications. The use of benign or non-toxic solvents is not trivial since most solvents used for the electrospinning process are very effective in dissolving polymers, providing desirable solution properties for electrospinning, but they are highly toxic for both the operator and the environment. Moreover, residual traces can compromise cell viability.

Different ratios of PCL-zein / crosslinked zein were explored. The best electrospinning parameters were adjusted to each composition and solvent. All the fibers were characterized and the composition with the best properties was used to produce aligned electrospun fibers to mimic the native structure of the tendon.

Through the analysis of these assays, promising results were obtained with PCL/ZEIN blends at a ratio of 2:1. Aligned fibers displaying characteristics suitable for use in tendon tissue engineering were produced with these blends.

Resumen

Los andamios son materiales de soporte utilizados en aplicaciones de ingeniería de tejidos para reparar o restaurar tejidos dañados, proporcionando un entramado tridimensional temporal o permanente para que las células crezcan, se diferencien y regeneren el tejido dañado. Estos andamios actúan como soporte estructural, guiando la formación de nuevo tejido mientras promueven la adhesión celular, proliferación y difusión de nutrientes.

Los andamios desempeñan un papel vital en la ingeniería de tejidos y la medicina regenerativa, facilitando el desarrollo de tejidos y órganos funcionales para trasplante o propósitos terapéuticos. Los investigadores adaptan las propiedades de estos andamios, incluyendo su porosidad, resistencia mecánica y tasa de degradación, para adaptarse a tipos de tejidos específicos y la aplicación prevista. El uso de células madre en los andamios permite dirigir la proliferación celular y regenerar tejidos en direcciones específicas. Los andamios son compuestos por diferentes tipos de biomateriales, incluyendo biopolímeros, polímeros sintéticos, biocerámicas y metales biodegradables. La combinación de polímeros sintéticos y naturales puede superar algunas desventajas de cada uno y producir nuevos materiales con propiedades superiores.

Además, los andamios pueden combinarse con varios factores biológicos como factores de crecimiento, citocinas o incluso células madre para mejorar aún más la regeneración de tejidos. Al integrar estos elementos bioactivos, los andamios pueden estimular actividades celulares específicas, modular el microambiente del tejido y promover una cicatrización y remodelación tisular más efectivas.

Este proyecto presenta un estudio sobre la fabricación y caracterización de andamios basados en poli(ϵ -caprolactona) (PCL) y zeína / zeína entrecruzada preparados mediante la técnica de electrohilado verde. Se utilizó un sistema de solventes benignos (ácido acético/etanol). La zeína es una proteína vegetal ampliamente disponible, biodegradable y biocompatible con un creciente interés como vehículo para una amplia variedad de aplicaciones biomédicas. Sin embargo, su pobre rendimiento mecánico requiere la combinación con polímeros biocompatibles sintéticos para preparar andamios adecuados para aplicaciones de ingeniería de tejidos. El uso de solventes benignos o no tóxicos no es trivial ya que la mayoría de los solventes utilizados para el proceso de electrohilado son muy efectivos en la disolución de polímeros, proporcionando propiedades de solución deseables para el electrohilado, pero son altamente tóxicos tanto para el operador como para el medio ambiente. Además, las trazas residuales pueden comprometer la viabilidad celular.

Se exploraron diferentes proporciones de PCL-zeína/zeína entrecruzada. Los mejores parámetros de electrohilado se ajustaron a cada composición y solvente. Todas las fibras fueron caracterizadas y se utilizó la composición con las mejores propiedades para producir fibras electrohiladas alineadas para imitar la estructura nativa del tendón.

A través del análisis de estos ensayos, se obtuvieron resultados prometedores con mezclas de PCL/ZEINA en una proporción de 2:1. Se produjeron fibras alineadas que muestran características adecuadas para su uso en la ingeniería de tejidos tendinosos con estas mezclas.

2. Introduction

2.1. Tendon

Tendons connect muscle to bone and their function is to transmit the force created from the muscle to the bone, making possible the movement. They are soft and fibrous tissues with high resistance to mechanical loads to resist uniaxial tension, but also have viscoelastic properties with good flexibility and optimal elasticity. This allows the conduction, distribution, and modulation of internal forces exerted by the muscles to the structures at the same they resist external forces from direct contusions and pressure, reducing possible damages on the tendon.

The tendon composition and their particular structure in the extracellular matrix (ECM) gives them these exceptional properties. The correct orientation of the collagen molecules confer high mechanical strength, meanwhile the breaking strength is related to their thickness and collagen content. The configuration and behavior of collagen fibers varies depending on the stress to which they are subjected.

In a typical stress-strain curve, three different zones can be seen as shown in Figure 1. The first zone is called toe region and is maintained until the strain reaches 2%. At rest, collagen fibers and fibrils have a crimped configuration that acts as a buffer against fiber damage, and appears only when the stress is released. This curled configuration decreases as tension increases. [1] Then comes the region of linear deformation, where the tendons behave elastically, with a constant slope that represents the stiffness or Young's modulus. This behavior is due to intramolecular sliding that arrange the fibers in parallel. Up to approximately 4% strain, the tendons return to their original length when the stress is released. Beyond this point, microscopic damage to the fibers can occur, leading to strains in the crimped configuration and generating changes in the stress-strain curve. At deformations between 8% and 10%, there are macroscopic failures of the fibers leading to tissue rupture. [1]

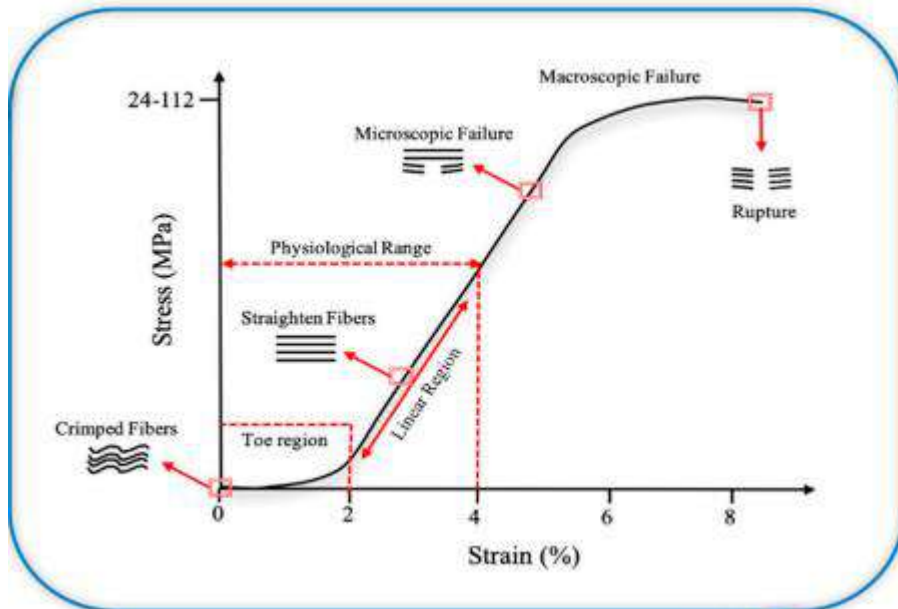


Figure 1: Stress-strain curve for tendon [1]

2.1.1. Tendon structure

The tendon is mostly composed of collagen, a stiff structural protein which provides the tissue a considerable tensile strength. The collagen molecules are arranged in a hierarchical manner and interspersed with a less fibrous and highly hydrated matrix, usually called ground substance.

Briefly, this structure starts with the crosslink of tropocollagen molecules on soluble form in order to produce insoluble collagen molecules that gradually aggregate into defined units referred to as collagen fibrils. A twisted bundle of collagen fibrils makes a collagen fiber, and the aggregate of collagen fibers form a fascicle [2]. A fine sheath of connective tissue surrounds the fascicle binding the fibers together. The objective is to surround the tendons in regions away from joints, to facilitate movement of tendons below the skin [3]. This hierarchical structure is shown in Figure 2.

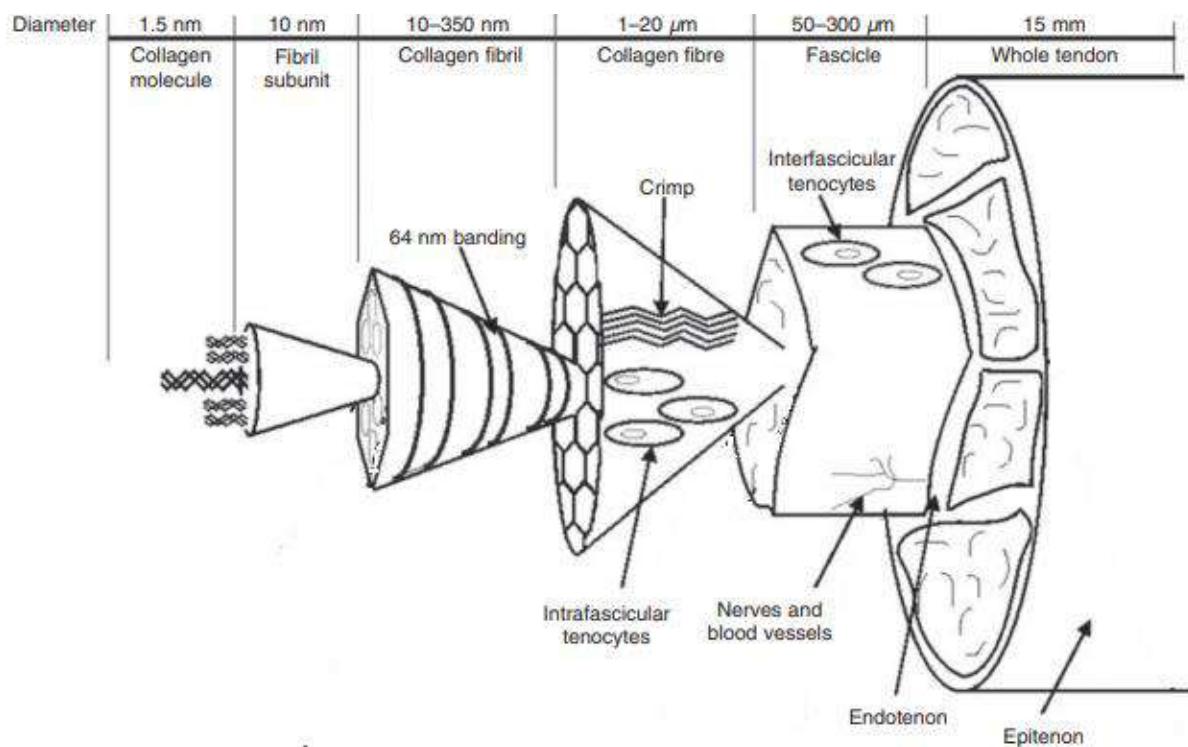


Figure 2: *Tendon structure from collagen molecules to the whole tendon [4]*

In addition to collagen, the ECM is composed of ground substance and elastic fibers. The elastin is the most abundant and core protein, they are a key structural constituent of tendon due their properties as high elasticity, fatigue resistance and store and return energy [2]. Are responsible for maintaining structural integrity and elasticity, allowing the tissue to return to its original shape once the tensile force is removed.

In the ground substance the most abundant tendon non-fibrous protein is proteoglycan, and the most abundant and well characterized of this is decorin. They have a key role in tendon development, it is bound to adjacent collagen fibrils, forming an interfibrillar bridge. [3]

Analyzing the microstructure of the tendon, 90-95 % of the cellular elements are tenoblasts and tenocytes. Tenoblasts are mainly present in young tendons, they are immature cells that give rise to round tenocytes during maturation and aging [3]. These are fully differentiated cells that are typically anchored to collagen and located throughout the tendon tissue, forming a kind of complex red cytoplasm. This allows them to exchange ions and small molecules, ensuring electrical plugging and facilitating the diffusion of signaling and nutrients into this poorly vascularized tissue. This gap junction communication also allows tendons to coordinate synthetic

responses to mechanical stimuli [2]. For all this they have a key role in the growth, maintenance, synthesis and turnover of the ECM, homeostasis and repair of the tendon.

2.1.2. Tendon wounds

Tendon wounds are very common in adults or in high performance athletes. Starting a physical activity without an adequate warm-up or a force performed incorrectly may lead to partial or complete breaks. But also the problems increase with the aging, due to elastin content being reduced which contribute to increasing tendon stiffness and reduce its resilience [2]. These injuries are a problem because they are used to be ignored or misdiagnosed. A contusion or laceration may lead to the fracture of a bone or a dislocation, taking all the attention of the doctors and, for example, ignoring ruptures of interphalangeal tendon joints may not be treated properly. [5]

On the other hand, an indirect trauma can occur due to a traction overload. Tendons can withstand higher tension forces than muscles and bone attachment sites. When ruptures occur in the midsubstance of the tendon, they are usually due to some pre-existing degeneration, such as loss of tenocytes, loss of cell structure or decreased collagen content, etc. [6]

Chronic wounds, together with inflammation and its subsequent repair make them susceptible to fibrosis. The accumulation of the components of the extracellular matrix, in this case collagen, leads to the formation of fibrotic scar tissue. [9] This scar tissue has the characteristic of a decrease in the mechanical properties with respect to the original tissue, being susceptible to future injuries.

2.1.3. Tendon regeneration

For adults, tendon injuries are a problem due to the low regeneration of the tendon tissue. Adult tendons have a limited natural healing capacity due to the low vascularization, the hypocellularity, the anisotropy and the non-linear mechanical properties of these tissues. In addition, it may not respond as expected to current treatments such as rehabilitation, drug delivery or surgery [7]. New approaches for regeneration are based on cell therapy and tissue engineering, through a combination of transcription factors, growth factors, and mechanical stimulation propose a long-term solution. The recovery of the microstructure and biomechanical properties of the tissue is the key point, also avoiding the formation of scar tissue.

2.2. Tissue engineering of tendon

Sometimes, artificial implants are not a proper solution due to their finite useful life. The human body is an aggressive environment leading to their degradation, loss of mechanical properties and inability to fulfill the function for which they were designed. In the case of tendon tissue engineering, carbon fibers and Dacron grafts are the most widely used materials, but none can match the adaptability and flexibility shown by functional tissues, which are also constantly self-remodeling. [10] In response to these problems, tissue engineering arises.

Tissue engineering (TE) is a branch of engineering that combines fields such as biomaterials, bioengineering, and cell biology with the aim to regenerate tissues damaged by injury, disease, or defects. Extracting cells from the patient's tendon and expanded in a cell culture and seeded onto a carrier. The highly porous scaffold combined with the use of stem cells are complemented with mechanical and biochemical stimulation, allowing driving cells to proliferate and regenerate tissues in specific directions [1]. An approximate scheme of this technique can be seen in Figure 3. This tissue, being the patient's own, does not generate an immune response from the body, avoiding one of the potential problems of using an external implant.

The main challenge of tendon tissue engineering is to replicate the mechanical properties of the tendon, their structure allows them to withstand non-linear mechanical deformations. Therefore, the key is not to find a material to replace the tendon, but to induce the repair of small defects and the induction of tissue self-regeneration. [10]

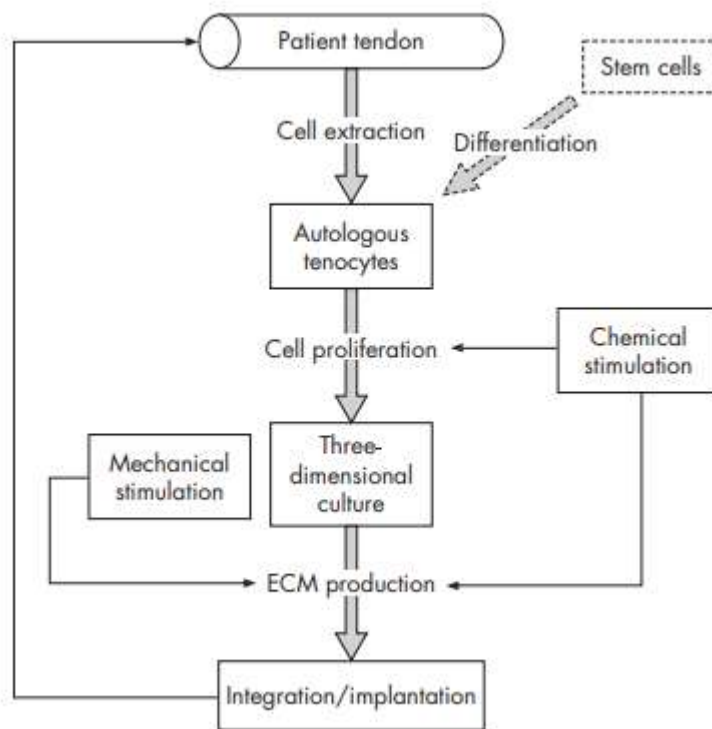


Figure 3: Scheme of tissue engineering for tendon *in vitro*, starting from the autologous cells of the patient [10]

2.2.1. Scaffold for tendon regeneration

Scaffolds have a series of generalities to fulfill their role in TE. They must support the cells and possess sufficient mechanical strength to withstand handling upon implantation in the human body. Its manufacturing is also important, since the scaffold must be scalable, as well as having economic and clinical viability that allows its commercialization. Going into more detail, there are a series of characteristics that the scaffold must have for tendon regeneration::

Biocompatibility: Scaffolds can be made from a natural or synthetic material, the key is to select one or a combination of materials that are biocompatible with the human body. This means that the cells are allowed to grow, penetrate and proliferate throughout the entire structure. In addition, biocompatibility allows preventing or minimizing the body's immune response. Otherwise the area becomes inflamed, compromising the chances of regenerating correctly and there is even a risk of rejection.

Biodegradability: It is a crucial aspect of scaffolds used in tissue engineering applications. These scaffolds are intentionally designed to be temporary, meaning they can be broken down and absorbed by cells and bodily fluids over time. However, the rate of degradation is a critical factor in the success of the scaffold.

Ideally, the degradation rate should be carefully controlled. It must be slow enough to allow cells to reproduce and replace the scaffold with natural collagen, which is vital for the formation of new tissue. At the same time, the scaffold should gradually disappear as the new tissue takes over the mechanical load. If the scaffold degrades too quickly, it may not provide enough support for proper tissue growth and could compromise the overall success of the tissue regeneration process.

Moreover, the scaffold degradation products must be non-toxic to avoid harmful effects on the body. Additionally, these products should be easily reabsorbed or removable by the body to prevent any adverse reactions or complications.

In summary, the biodegradability of scaffolds is a delicate balance. It must allow for gradual tissue regeneration while ensuring that the scaffold itself does not impede the development of the new tissue. Furthermore, the degradation products must be biocompatible and pose no harm to the body, contributing to the overall success and safety of tissue engineering applications.

Mechanical Properties: Scaffolds must be specifically designed to have mechanical properties within the usual ranges for a tendon. The scaffold must provide the cells with sufficient rigidity, so they can produce collagen and proliferate, while allowing them to experience different levels of mechanical stimulation [7]. In addition, it must be slightly less strong and rigid than the host tendon so as not to induce damage to surrounding tissues at the time of suturing. Finally, it must possess a certain degree of ductility to prevent abrupt failure in the event of a tension overload.

Structure: The scaffold design should allow the cells to replicate the hierarchical structure of collagen in the tendon. This means that the architecture induces cells to adhere, grow and proliferate in the direction of fiber alignment. The desired morphology is acquired and with it the mechanical properties of the tissue to be regenerated.

Porosity: The structure must be porous so it is fully interconnected and the cells can penetrate and proliferate throughout the entire scaffold, promoting vascularization

and new tissue formation. The interconnection allows the diffusion and exchange of nutrients between the cells and the ECM, while allowing the release of waste and degradation products. [7] Lastly, the pores allow the mechanical properties to be manipulated in such a way that they match those sought by the fabric.

2.2.2 Materials for Tendon Tissue Engineering

It's hard to find a material that ticks all the boxes to make a scaffold for Tendon TE. To maximize the advantages of the materials, and complement their disadvantages, the use of scaffold composites is gaining more and more strength in the field of the TE tendon. These are combinations of two or more materials resulting in mechanical and biological properties that match with those of the tissue to be regenerated.

Polymers of natural origin such as collagen, silk or chitosan have a tendency to mimic the natural structure of the tendon and its properties. Collagen is a good platform because it is the main component of the tendon and it has excellent biocompatibility. The disadvantages are linked to its mechanical properties, since it has a high degradation rate and little structural stability, as well as immunological risks due to being of animal origin. Alternatives such as silk arise due to its exceptional mechanical properties in terms of strength, tenacity and elasticity. Now the problems are linked to its bioactivity, since it does not allow sufficient cell union or growth. Chitosan is also used due to the structural similarities with elements present in the ECM and is characterized by its biocompatibility, biodegradability, antibacterial capacity and non-toxicity. However, its low mechanical properties due to the rigidity of its membranes make its use difficult for this purpose [1].

On the other hand, the most interesting synthetic materials for use in Tendon TE are the bioresorbable ones, such as polyglycolic acid (PGA), polylactic acid (PLA) and polycaprolactone (PCL). Synthetic polymers have high inherent flexibility in synthesizing or modifying polymers matching the physical and mechanical properties. Considering their manufacture, they are mostly cheap, can be scaled up industrially, and their mechanical properties are reproducible from batch to batch. Some of the cons are the risk of rejection due to reduced bioactivity since they don't promote cell adhesion and growth. [1]

2.2.3 Proteins

Proteins are macromolecules made up of linear chains of amino acids. Proteins perform various functions and are differentiated according to the sequence of amino acids. They are used in fields such as TE due to their properties such as biocompatibility and biodegradability, non-toxicity, etc. On the other hand, other benefits are their availability on a large scale and low cost, at the same time they come from renewable sources.

Zein is a type of protein derived from corn (maize) and is considered a vegetal (plant-based) protein. It belongs to the prolamin family of proteins, which are a subgroup of storage proteins found in seeds of cereals like corn, wheat, and rice. As a plant protein, zein plays a significant role in various applications within the food and non-food industries.

In the context of proteins, zein is unique because it is relatively insoluble in water, which sets it apart from most other proteins. Instead, it is soluble in alcohol solutions, making it a valuable material for certain applications.

In the food industry, zein has gained attention as an alternative protein source due to its functional properties. It can be used to form edible films and coatings, providing a protective layer for foods, such as snacks, candies, and pharmaceutical products. The biodegradable nature of zein makes it an attractive eco-friendly option for packaging materials, replacing traditional plastic films.

Furthermore, zein can be utilized in the formulation of gluten-free food products, as it lacks the gluten proteins found in wheat and can help improve the texture and structure of gluten-free baked goods.

In the non-food sector, zein finds applications in various industries, including pharmaceuticals, cosmetics, and coatings. It is used as a binder in tablet formulations, a film-forming agent in cosmetic products, and a component in biodegradable coatings for pills and capsules.

As a vegetal protein, zein contributes to the growing trend of plant-based diets and sustainable alternatives to animal-based proteins. Its unique properties and versatile applications make it an exciting prospect in both the food and non-food

sectors, further diversifying the options available for protein utilization and promoting more sustainable practices.

Zein is a protein derived from corn, and it possesses several notable characteristics. Its isoelectric point is 6.2, which means it carries no net electrical charge at this pH level. One of the remarkable features of zein is its hydrophobic nature, making it difficult to dissolve in water under normal conditions. However, zein exhibits solubility in specific environments: it can dissolve in water when the ethanol concentration is between 60% to 95%, or in alkaline solutions with a pH above 11. The unique solubility behavior of zein can be attributed to its high content of hydrophobic amino acids, particularly Leucine and Alanine [12]. These hydrophobic amino acids tend to cluster together in the protein's structure, leading to its overall resistance to water-based solvents.

Due to its hydrophobic properties and limited solubility in water, zein finds practical applications in various industries. For example, it is used in the food industry to create coatings and films for confectionery products, providing a protective barrier. Zein is also employed as a biodegradable packaging material, serving as an eco-friendly alternative to conventional plastics. The chemical structure of zein can be seen in Figure 4.

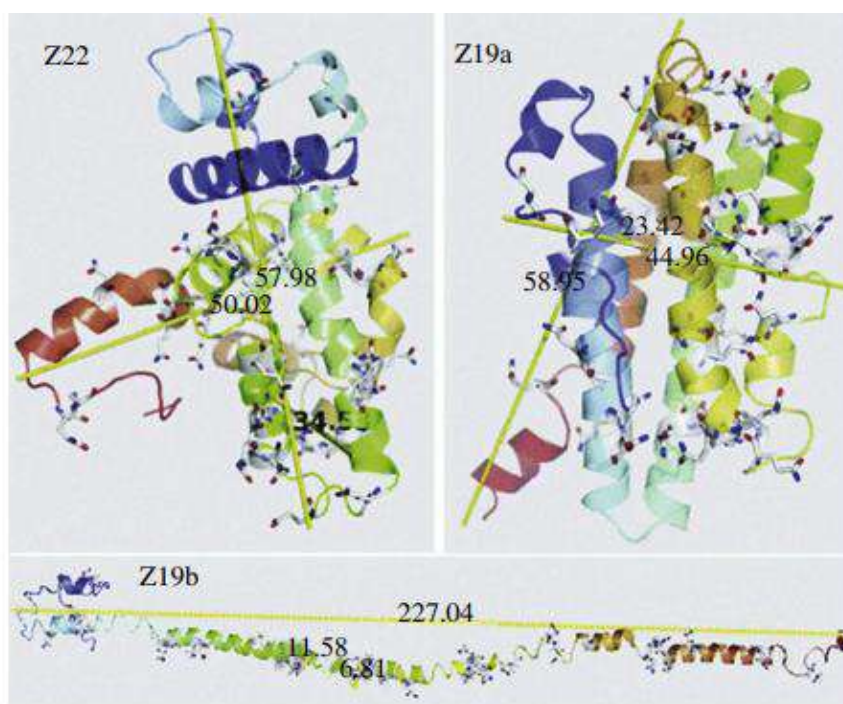


Figure 4: *Cartoon illustrations of structure models of zein according to Li et al. [17]*

Zein is a natural polymer that exhibits enhanced interactions with cells, primarily through its interactions with membrane receptors. Its plant-based origin offers several advantages over proteins derived from animals. For instance, using zein reduces the variability found in different batches, minimizing the risk of disease transmission or immune responses that may occur with animal-based proteins. Furthermore, the use of zein aligns with the growing trend of reducing the reliance on animal resources in research and development. By opting for vegetal proteins like zein, we contribute to the ethical and sustainable approach of minimizing animal usage in scientific investigations.

In tissue engineering (TE) applications, zein exhibits several advantageous properties, such as resistance to microorganisms, flexibility, compatibility with the human body, and biodegradability. However, there are some limitations to consider. Despite its biodegradability, zein has a relatively high degradation rate, which can be problematic for certain tissue engineering scaffolds. Additionally, its mechanical properties may not be sufficient to provide the necessary structural support for certain tissue regeneration processes.

Because of these factors, using zein alone to create a scaffold may not be ideal. However, researchers and engineers often overcome these limitations by combining zein with other materials or by modifying its structure to improve its mechanical strength and stability. For example, zein can be blended with other biocompatible polymers or reinforced with materials like nanofibers or nanoparticles to enhance its mechanical properties and slow down its degradation rate.

By leveraging zein's beneficial properties and addressing its drawbacks through strategic combinations and modifications, it is possible to develop scaffolds that promote successful tissue regeneration and repair. This approach allows for the harnessing of zein's advantages while mitigating its limitations, making it a valuable component in the broader field of tissue engineering.

2.2.4. Synthetic polymers

Synthetic materials often have exceptional mechanical properties, but they tend to fail at promotion of cell attachment and proliferation. It is a good idea to use a synthetic polymer and combine it with a protein so that the scaffold acquires some hydrophilicity and improves cell viability, while maintaining its structural properties. [12]

Poly(ϵ -caprolactone) (PCL) is a semicrystalline, aliphatic, and hydrophobic polyester with excellent mechanical properties, good biocompatibility and electrospinnability in organic solvents. In addition, it has a low toxicity, this is because it degrades for hydrolysis of ester bonds into acidic monomers, which can be removed easily from the body. [13]. The chemical structure of PCL is shown in Figure 5.

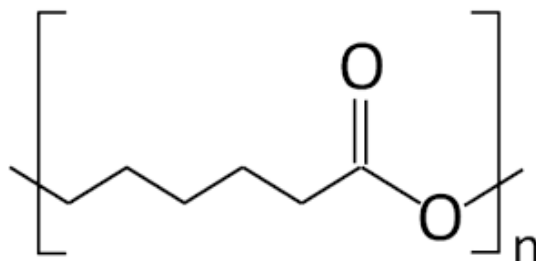


Figure 5: Scheme of PCL chemical structure

However, some of its limitations are that its high crystallinity gives it a slow degradation rate, in addition to being hydrophobic, which makes cell attachment and penetration into the porous structure difficult. Also, some side effects can be seen due to the acidic degradation products.

2.3. Electrospinning technique

Electrospinning is a technique that has gained popularity in recent years in the field of tissue engineering (TE) due to its ability to easily produce scaffolds. This method utilizes an electric field to produce nano or micrometric polymeric fibers, creating porous and versatile structures [14].

The process of electrospinning requires a few essential elements to carry it out effectively:

- A reservoir containing a suitable polymeric solution, typically a syringe with a needle attached.
- A syringe pump to control the flow rate of the polymeric solution.
- A metal collector connected to the ground, which serves as the substrate for the fibers to be collected on.

- A high voltage source with two electrodes, one connected to the metal needle (usually the positively charged electrode) and the other to the collector (often the negatively charged electrode).

When the high voltage is applied to the polymer solution, it forms a charged jet that undergoes elongation and whipping motions, eventually resulting in the solidification of the polymer fibers as they are collected on the metal substrate. This electrospinning technique offers several advantages, such as the ability to create scaffolds with fine fibers and high surface area-to-volume ratios, making them suitable for supporting cell attachment, growth, and tissue regeneration in TE applications.

The high voltage power source induces charge of polarity in the polymer solution. The solution is slowly pumped out of the needle tip towards the collector with the opposite polarity. Initially, the droplet is spherical but soon the surface is covered by charges of the same sign and with the repulsion among these charges destabilizes the spherical shape. When the repulsion is strong enough to overcome the surface tension, the droplet deforms into a conical shape (called Taylor cone), and a fiber jet is ejected from the cone [7]. The repulsive forces cause the whipping of the liquid jet, evaporating the solvent on the atmosphere, to finally deposit solid fiber on the collector. The result of this process is the formation of fibers with an adjustable morphology, diameter and orientation.

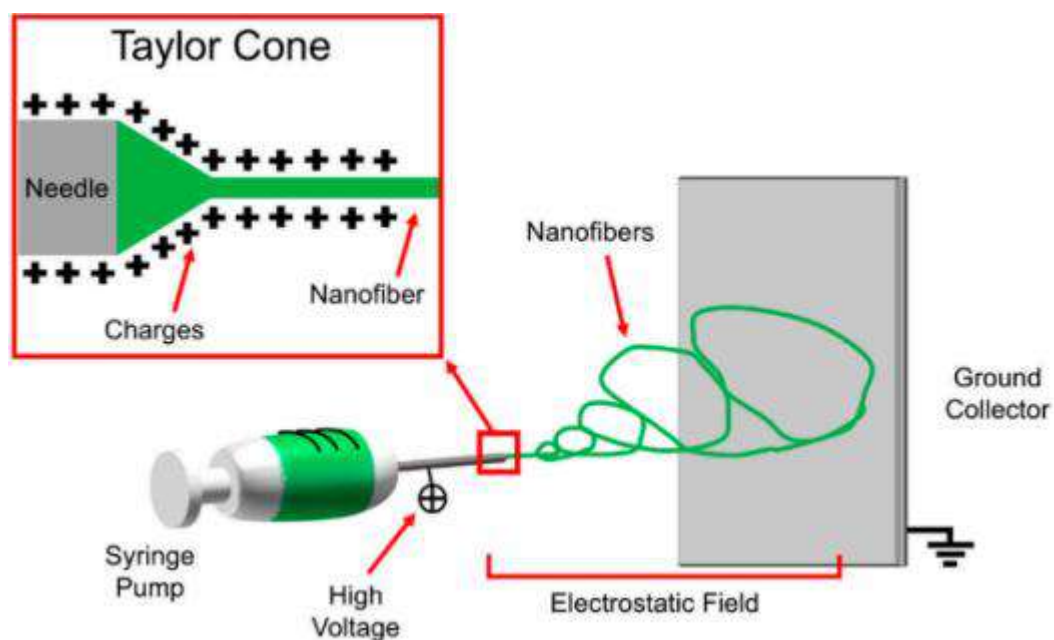


Figure 6: *Electrospinning operating principle and Taylor cone formation [7]*

The type of collector is one of the most important parameters of the technique since it controls the final structure of the fibers. Static flat collectors (Figure 7.A) allow the formation of nanofibrous mats, a drum collector rotating at low speed, producing random nanofibers (7.B). But a high-speed rotating drum (7.C) forms aligned fibers which are interesting for tendon TE.

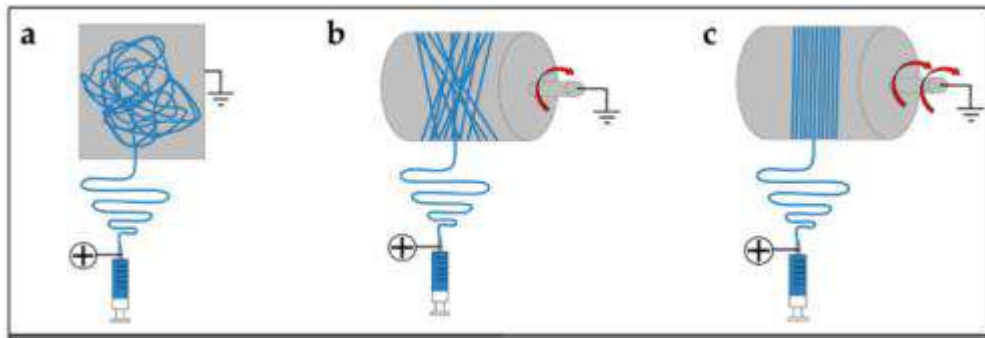


Figure 7: Different electrospinning collector: (a) flat plate collector; (b) drum collector rotating at low speed, producing random nanofibers; (c) drum collector rotating at high speed, producing aligned nanofibers. [7]

2.3.1. Solution Parameters

The solution parameters are directly linked to the polymer and the solvent, as both components play crucial roles in the electrospinning process, resulting in the formation of polymer fibers. The spinnability of the solution is determined by its ability to form continuous and uniform polymer fibers. The solution's composition and properties influence the electrospinning process, affecting the fiber's morphology, diameter, and overall quality.

The choice of polymer is essential, as it determines the mechanical properties, biocompatibility, and degradation characteristics of the resulting scaffold. Different polymers have varied solubility in solvents, affecting the solution's viscosity, surface tension, and conductivity, which are critical parameters in electrospinning.

Similarly, the solvent used in the polymer solution significantly impacts the electrospinning process. The solvent's volatility and polarity influence the rate of solvent evaporation during fiber formation, directly affecting the fiber's morphology, diameter, and alignment. Proper solvent selection is crucial to achieving the desired fiber characteristics and scaffold properties.

Maintaining optimal solution parameters is essential for achieving uniform fibers and preventing defects in the final scaffold. Variations in solution composition, viscosity, or conductivity can lead to uneven fiber deposition, bead formation, or inconsistent fiber diameters, which may impact the scaffold's mechanical strength and cellular response.

2.3.1.1. Viscosity / concentration of polymer solutions:

The viscosity is strictly related to the concentration of the polymer. The concentration of the polymer must be enough to allow the polymer chains to entangle and form the fibers. However, if the concentration is too high, the viscosity increases and a constant flow of solution cannot be achieved. On the other hand, a low concentration of polymer causes the fibers to break before reaching the collector.

2.3.1.2. Conductivity of solvents and polymers:

Solutions with high conductivity will have a greater capacity to carry charges, so the fibers will be subjected to greater tension and their diameter will reduce. In addition, insufficient conductivity causes the fibers to not elongate sufficiently, therefore uniform fibers are not achieved and the number of beads present increases [14].

2.3.1.3. Polymer-solvent systems:

The solvent must dissolve the polymer and be volatile enough to allow its own evaporation, otherwise the presence of solvent-containing nanofibers on the collector will cause the formation of beaded nanofibers [7]. But a too volatile solvent causes the drying of the jet at the needle tip, blocking the electrospinning process.

In addition to these parameters, the choice of a polymer-solvent system involves other external factors. Most solvents used for the electrospinning process are very effective in dissolving polymers and providing desirable solution properties for electrospinning, but they are also hazardous for the operator and the environment. If the idea is to get involved in new approaches such as green electrospinning, the polymer-solvent system will have to change. This current of more eco-conscious working, uses “safe” solvents or class 3 solvents according to ICH classification. Some examples are acetic acid, formic acid, acetone, etc.

2.3.2. Processing parameters

2.3.2.1. Flow rate:

Lower flow rate often results in smaller diameter fibers, but if it's too low the Taylor cone is not stable and may lead to defects. On the other hand, the higher the flow there is an increase in the diameter of the fibers, as well as the possibility of laying beads in the final product because the solvent has less time to evaporate.

2.3.2.2. Voltage:

Voltage is one of the most critical parameters in the electrospinning process, and its influence is dependent on the viscoelastic properties of the solution. As a result, each polymer-solvent system has an optimal voltage range. Typically, higher voltages lead to the formation of larger fiber diameters, but this relationship is not always linear and may depend on other process parameters. However, it's important to note that using higher voltages can also lead to the occurrence of defects in the fibers, such as the formation of beads. This is primarily due to the instability of the Taylor cone, which can be exacerbated when the voltage is too high. Beads and irregularities in the fibers can adversely affect the scaffold's mechanical properties and overall functionality.

On the other hand, if the voltage is not sufficient, a fiber jet may not form because the charges in the solution do not overcome the surface tension forces [15]. In this case, the electrospinning process may not be successful, and fiber formation will not occur.

2.3.2.3. Distance between needle and collector:

The distance between needle and collector determines the morphology of the fibers. In general, large-diameter nanofibers are formed when the distance is small, whereas the diameter decreases as the distance is increased [7]. Also the distance must be enough to allow the solvent to evaporate, otherwise the presence beads can be observed.

3. Objectives

The main objectives of this work are:

- To fabricate electrospun zein-based fibrous scaffolds for tendon tissue engineering by using benign solvents for the electrospinning process.
- To optimize processing parameters for the production of electrospun PCL / zein based scaffolds
- To determine the mechanical properties of the obtained PCL / zein based electrospun mats.
- To characterize the composition, morphology and surface properties.
- To investigate the degradation behavior of PCL / zein electrospun fibers
- To assess the in vitro cell behavior of the scaffold.

4. Materials

Poly(ϵ -caprolactone) (PCL) ($M_n = 80.000 \text{ g.mol}^{-1}$) and zein (CAS No: 9010-66-6) were used. Acetic acid was used as a solvent in the PCL / zein blends and ethanol with N-(3-dimethylaminopropyl)-N'-ethylcarbodiimide hydrochloride (EDC) and N-hydroxysuccinimide (NHS) was used as a crosslinker agent for zein. All materials and reagents were purchased from Sigma Aldrich, Germany.

From now on, the samples will be named as follows:

Zein AA: Zein non-crosslinked (with acetic acid as solvent)

Zein CC: Zein crosslinked with EDC and NHS (with ethanol as solvent)

PCL / zein: PCL / zein blend (ratio: 1:1,1:2,2:1)

PCL: poly(caprolactone) mats (prepared with acetic acid as solvent)

4. Methods

4.1. Fabrication of electrospun scaffold

Four types of nanofibrous mats were prepared using electrospinning technique: crosslinked and non crosslinked zein mats, PCL mats and blends of PCL/zein. Figure 8 shows the equipment used in this work. In all the different experiments the reservoir was a plastic syringe with a stainless steel needle of 21 G.



Figure 8: *Electrospinning equipment (Starter Kit 40KV Web) with a flat collector. Friedrich-Alexander-Universität Institute of Biomaterials (Erlangen, Germany)*

For the preparation of crosslinked zein mats (Zein CC), the procedure reported by L. Vogt was followed [16]. The electrospun solution was zein 26 wt% in ethanol 90% (1 part distilled water, 9 pure ethanol) + 60 mg of EDC and 60 mg on NHS per gram of zein in the solution. First, the zein was dissolved for 15 min, and then EDC/NHS was added for crosslinking. In this way, 3 types of samples were prepared, those that were stirred for 1 h, for 24 h and 72 h. The processing parameters were the same for all the runs, a flow rate of 0.7 mL/h with an applied voltage of 20 kV, while the needle-tip to aluminum collector distance was maintained at 10 cm.

Uncrosslinked zein mats of 30% wt with acetic acid were also prepared (Zein AA). Following the procedure reported by A. Massone [21]. In this case the electrospinning was carried out at a flow rate of 0.8 mL/h with an applied voltage of 15 kV. The needle-tip to aluminum collector distance was maintained at 15 cm.

On the other hand, working only with PCL, the fiber of mats were prepared by dissolving the PCL (20% wt) in the acetic acid solvent. The flow rate was 0.4 mL/h with an applied voltage of 15 kV. The needle-tip to aluminum collector distance was maintained at 15 cm.

For the preparation PCL / zein blends, PCL 20% wt was added to a solution of 10 ml acetic acid and then zein 10%wt was added. The flow rate was 1.4 mL/h with an applied voltage of 15 kV. The needle-tip to aluminum collector distance was maintained at 15 cm.

In the second case, PCL / zein blends with a ratio of 1:1 were also prepared following these preparation procedures. The flow rate was 0.8 mL/h with an applied voltage of 15 kV. The needle-tip to aluminum collector distance was maintained at 15 cm.

The last PCL / zein blend, with a ratio of 1:2, was also prepared following these procedures. The flow rate was 0.3 mL/h with an applied voltage of 20 kV. The needle-tip to aluminum collector distance was maintained at 15 cm.

In Figure 9 (a) on the left, a flat collector was used, resulting in a mat of fibers. The fiber composition used was PCL/zein in a ratio of 2:1. Similarly, the same composition of fibers was electrospun using a drum rotating collector with the same parameters. The right picture (b) shows that aligned fibers were obtained with this setup.

Finally, five samples of each composition were obtained using the flat collector, and an extra sample of PCL / zein 2:1 was prepared with a rotating collector. The experiments had a duration of 2 h aiming for a thickness that would enable easy manipulation and experimentation. Table 1 shows the different parameters and post-processing conditions for the used solutions.



Figure 9: The influence of collectors on the final structure of the fibers. (a) typical random fibrous mat, (b) aligned fibers.

Polymer	Solvent	Solution Concentration	T (°C)	RH	Voltage (kV)	Distance (cm)	Flow Rate (mL/h)	Spinning Time (h)
Zein CC (1 h stirring)	Ethanol 90%	26% wt + EDC/NHS	23.9	36%	20	10	0.7	2
Zein CC (24 h stirring)	Ethanol 90%	26% wt + EDC/NHS	24	30%	20	10	0.7	2
Zein CC (72 h stirring)	Ethanol 90%	26% wt + EDC/NHS	24.1	41%	20	10	0.7	2
Zein AA	Acetic acid	30% wt	23.5	48%	15	15	0.8	2
PCL / zein 2:1	Acetic acid	20% wt PCL + 10% wt zein	23.7	33%	15	15	1.4	2
PCL / zein 1:1	Acetic acid	15% wt PCL + 15% wt zein	23.8	38%	15	15	0.8	2
PCL / zein 1:2	Acetic acid	10% wt PCL + 20% wt zein	24.3	44%	20	15	0.3	2
PCL	Acetic acid	20% wt	23.9	45%	15	15	0.4	2

Table 1: Parameters of electrospinning

4.2. Microstructural and morphological characterization

4.2.1. Scanning electron microscopy (SEM)

All samples were examined with a scanning electron microscope (SEM) (Auriga-Base 0750 Zeiss, Germany) with 1 keV electron beam power. Mats were examined before the degradation test, and the most compromising formulations were examined after degradation.

The samples were placed in small plates and carefully cut to avoid modifying the surface and to maintain a realistic image (Figure 10). Mean diameter and diameter distribution of the fibers of different compositions were determined by using Image J (NIH, USA). The analysis of microstructure and morphology was performed to characterize the different fiber compositions and to select the most promising formulation for the preparation of aligned fibrous mats.



Figure 10: *Plates for samples for SEM examination*

4.2.2. Fourier transform infrared spectroscopy (FTIR)

The FTIR was performed with a IRAffinity 1S-Shimadzu (Kyoto, Japan) in absorbance mode, at the wavenumber ranging from 4000 cm^{-1} to 400 cm^{-1} , with a resolution of 4 cm^{-1} . Spectra analysis (band assignment) was carried out with the raw materials and the different scaffolds to characterize sample composition.

4.2.3. Mechanical tests

Uniaxial tensile tests of all the samples were performed, except on ZEIN CC samples because they were too brittle and break when setting them up. Three samples of each composition were tested, all samples were tested before degradation. The fibrous mats were removed from the aluminum film and cut into strips approximately 3 cm length and 5 mm wide. Samples were supported in 4 cm paper frames and attached with grips, Finally, frame edges were cut. By following this strategy, fibrous mats can be more easily handled and tested (Figure 11). Tests were carried out with a crosshead speed of 5 mm/min.

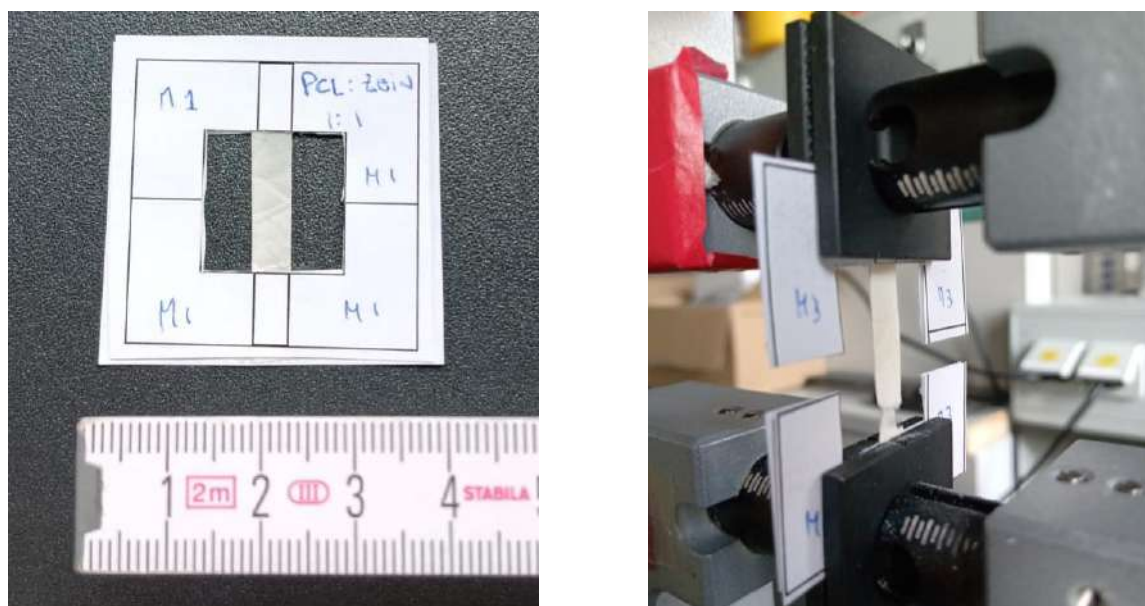


Figure 11: *Set up of the mechanical test*

4.2.4. Contact angle measurements

Contact angle measurements were carried out using a drop shape analyzer (DSA30 Expert, Krüss, Germany). The samples were cut and placed in a platform (Figure 12). All the tests were performed at room temperature, using water droplets to evaluate the hydrophilicity of fibrous samples. Approximately ten measurements were taken for each sample and the obtained results were averaged. Finally, using the DSA4 software, images were analyzed and the data reported.



Figure 12: *Fibrous mats with water drops during contact angle tests*

4.3. Degradation Test

Degradation tests were performed in PCL/Zein samples with 2:1 ratio (non aligned fibers). Twelve discs with a diameter of 1.5 cm were cut, detached from aluminum foil and weighed before starting the tests (initial dry mass). Then, samples were placed in individual flasks with 10 ml of PBS solution (pH=7.4). The composition of the PBS solution was NaCl 1.2 g, KCl 0,03 g, Na₂HPO₄ 0.213 g, KH₂PO₄ 0.036 g in 150 mL water. Flasks were placed in an incubator (Imperial III radiant heat incubators 302-1, Lab Line Instruments INC, USA) at 37°C (body temperature) with mild shaking (150 rpm) for 1, 7, 14 and 28 days. Samples were then removed from flasks, weighted (recorded as “swollen mass”), and dried with tissue paper. After that, they were dried under vacuum for a period of 72 hours and weighed again (recorded as “dry mass”). Finally, water uptake and weight loss were calculated at different periods of time using Equations 1 and 2, respectively.

$$\text{Water uptake (\%)}: \frac{m_w - m_i}{m_i} \times 100 \quad (\text{Equation 1})$$

$$\text{Weight loss (\%)}: \frac{m_i - m_d}{m_i} \times 100 \quad (\text{Equation 2})$$

m_i = initial mass ; m_w = wet mass; m_d = dry mass;

4.4. Cell Test

Cell viability assay and ALP activity assay were conducted using Normal Human Dermal Fibroblasts (NHDF) cell line purchased from Promocell (Heidelberg, Germany). Dermal fibroblasts are reported to be similar to tendon cells according to their molecular profiling, thus exhibiting potential to differentiate into tenocytes, and representing a viable tool for tendon tissue engineering (Chu et al., 2020).

NHDF culture at passage P+23 was maintained in medium sized flasks at 37°C in humidified pCO₂ atmosphere. High Glucose Dulbecco's Modified Eagle Medium (DMEM HG; TermoFisher Scientific, Germany), supplemented with 10% v/v Fetal Bovine Serum (FBS), 1% v/v penicillin/streptomycin, 1% v/v L-glutamine, was chosen as suitable culture medium. At 70-80% confluency, once every 5-7 days, cells were splitted in a new flask following trypsin digestion.

4.4.1. Cell Viability (WST-8 in vitro assay)

For the cellular test, the WST-8 assay was conducted. It is a colorimetric assay measuring the absorbance of WST-8 formazan, a product resulting from the reduction of the water-soluble tetrazolium salt WST-8 catalyzed by mitochondrial dehydrogenases, therefore directly correlated to the amount of metabolically active cells cultured on the samples.

Three replicates of each sample type were cut using a 12-mm skin biopsy punch, and carefully placed on the bottom of 24-well plates. The sample types consisted of randomly oriented PCL/zein 2:1, 24h-crosslinked zein, aligned PCL/zein 2:1. PCL 20% was used as a positive control while WST-8 in DMEM HG as a blank. The samples and the plate were sterilized using UV light under a working bench for 30 minutes per side. For the biological testing, 1.8×10^4 NHDF were seeded onto well plates containing the samples for each time-point considered, 24 hours and 7 days, and the well plates were stored in an incubator at 37°C with a humidified 5% pCO₂ atmosphere. At each time-point, 10 µL (1% v/v) of WST-8 solution, purchased from Sigma-Aldrich (Munich, Germany), were added to each well, and the plates were further incubated for 4 hours before transferring 100 µL from each well to another 96-well plate for the spectrophotometric measurement (FLUOstar-Omega BMG Labtech, Ortenberg, Germany) at 450 nm.

4.4.2. Cell Adhesion

To evaluate the morphology of the cells adhered to the materials investigated, the cells seeded onto the samples were dried through a critical point drying method, and examined via scanning electron microscopy.

In detail, after WST-8 was performed, the cell medium was removed from the well-plates containing the samples, and the cells were washed with PBS twice. Then, the cells were fixed through paraformaldehyde fixation, and immersed in ethanol dilution series (30%, 50%, 70%, 80%, 95% and twice 100%) for 30 minutes each. Lastly, samples were prepared for SEM analysis by critical point drying (Leica EM CPD300, Leica Biosystems, Wetzlar, Germany) and visualized as previously described.

4.4.3. ALP Activity

To evaluate the activity of ALP, a colorimetric assay based on p-nitrophenylphosphate (p-NPP) was performed. In fact, ALP is responsible for the hydrolysis of p-NPP to phosphate and para-nitrophenol (p-NP), whose amount can be measured at 405 nm, thus directly correlating the absorbance resulting from the presence of p-NP to the activity of ALP.

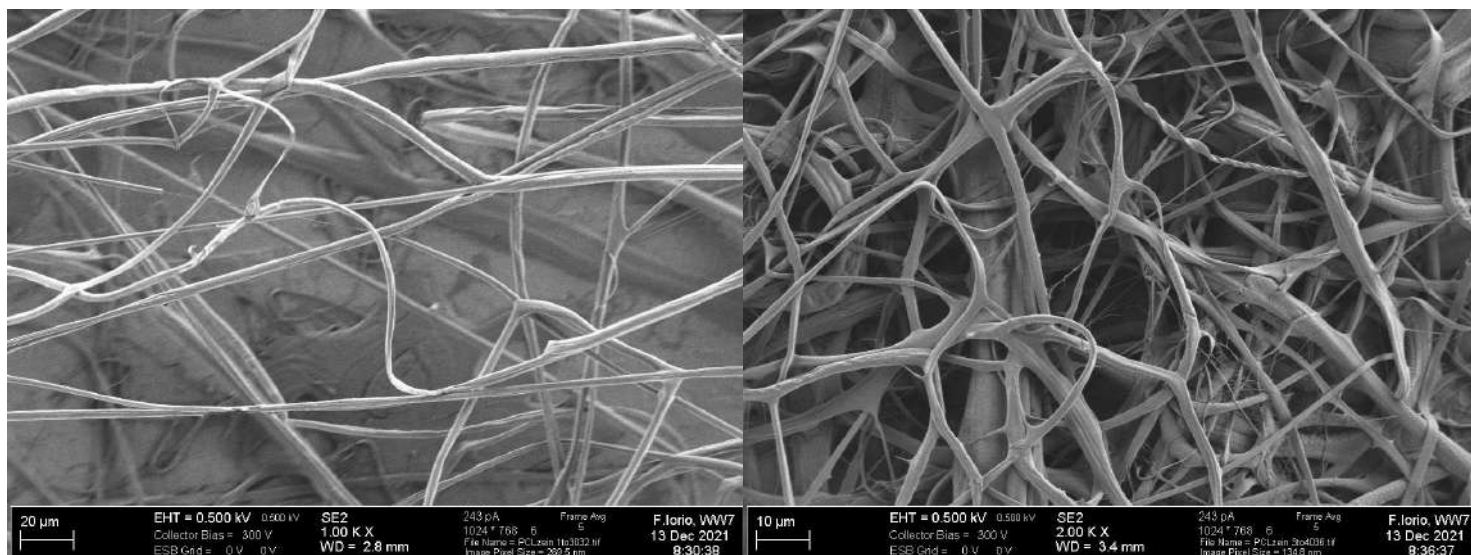
For the testing, 3 replicates of each sample type were cut using a 12-mm skin biopsy punch, and carefully placed on the bottom of 24-well plates. The sample types consisted of randomly oriented PCL/zein 5:1, PCL/zein 2:1, crosslinked zein, aligned PCL/zein 2:1. PCL 20% was used as a positive control while fresh DMEM HG as a blank. The samples and the plate were sterilized using UV light under a working bench for 30 minutes per side. Then, 1.8×10^4 NHDF were seeded onto well plates containing the samples for each time-point considered, 24 hours, 7 days and 14 days, and the well plates were stored in an incubator at 37°C with a humidified 5% pCO₂ atmosphere. At each time-point, cells were washed with PBS and lysed with 1% Triton X-100 for 30 minutes. The lysate was centrifuged at 2000 rpm for 5 minutes, then 250 µL of supernatant were transferred to a second 24-well plate. 100 µL of ALP-Mix (0.1 M Tri, 2 mM MgCl₂; pH adjusted to 9.8) containing 9 mM p-NPP were added to each well, and the reaction was left to occur in the dark for 4 hours. The reaction was stopped with 650 µL of 1M NaOH and the absorbance was measured spectrophotometrically (FLUOstar-Omega BMG Labtech, Ortenberg, Germany) at 405 nm and at 690 nm as a background.

6. Results and discussion

6.1 Fabrication of electrospun scaffold

The strategy of using blends of synthetic and natural polymers arises from combining the favorable mechanical properties of the synthetic component (a biocompatible polyester in this case) and the biocompatibility and hydrophilicity provided by the biopolymer. PCL is a bioresorbable polymer that degrades by hydrolytic mechanisms by breaking ester bonds, while zein is a vegetal protein obtained from corn, with interesting and attractive properties.

The first experiments were carried out using PCL:Zein ratio of 3:4 and 1:3. Unfortunately, the obtained mats presented numerous defects, as evidenced by SEM images in figure 13. After these results, in order to explore another PCL/zein system, the experimental conditions set in previous works were used [21].



A

B

Figure 13: SEM images of the samples. (A) PCL/Zein 1:3 (B) PCL/Zein 3:4.

In addition to these ratios and parameters, a PCL:Zein ratio of 1:2 was also studied, which contains a higher amount of Zein in search of better porosity and pore size. Additionally, Zein was cross-linked through EDC/NHS chemistry, which is a widely used chemical reaction in biochemistry and molecular biology for coupling carboxyl groups (-COOH) to primary amines (-NH₂) in molecules such as proteins, peptides, and nucleic acids. It is not toxic and also a zero-length crosslinker, which helps in forming bonds but is not included in the final crosslinked structure.

After preparing different samples, it was decided that the samples with a PCL/Zein 2:1 ratio would be the ones selected for the manufacture of aligned fibers. This was because removing the fibrous mats from the aluminum film was easier, thanks to the simplicity of sample handling.

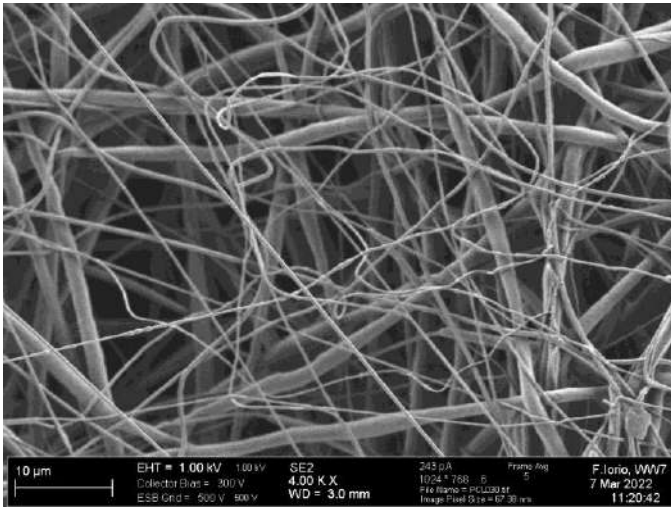
6.2 Microstructural and morphological characterization

6.2.1 Scanning electron microscopy (SEM)

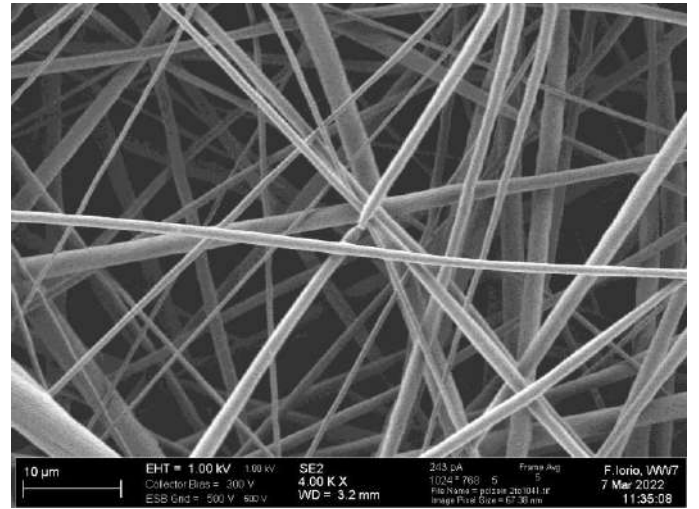
Figures 14 and 15 depict various types of samples prior to the degradation tests. In Figure 14A, a micrograph of PCL 20%, a rounded fiber morphology consisting of thick and fine fibers is observed. The structure is consistent with flawless fibers without beads.

Moving on to Figure 14B, PCL/Zein 2:1 shows a bead-free fiber mat composed of rounded and seemingly uniform nanofibers. Upon observing the 1:1 ratio of PCL/Zein in Figure 14C, a uniform fiber mat without beads is once again evident, albeit with a seemingly flatter morphology. In the case of the PCL/Zein 1:2 ratio (Figure 14D), a morphology similar to that of PCL 20% re-emerges. This morphology is characterized by large fibers interwoven with minute polymer strands. Finally, observing Figure 14 E, it can be seen that the aligned PCL/ZEIN 2:1 fibers exhibit a sort of bimodal structure. This is because the majority of the fibers are uniform and rounded in shape, but it appears that some of the fibers were fused together during the deposition process.

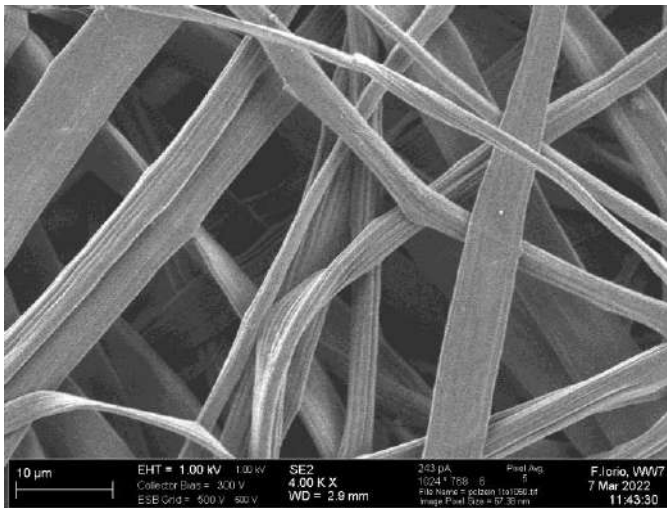
Zein AA (Figure 15.A) exhibited the smallest fibers distribution, displaying a rounded and apparently uniform morphology; however, they are marred by a significant number of beads that diminish their quality. On the other hand, Zein CC (Figure 15B, C, and D) consistently displays more flattened fibers with a uniform morphology. Notably, there are no significant differences among the samples prepared at 1, 24, and 72 hours before the spinning process.



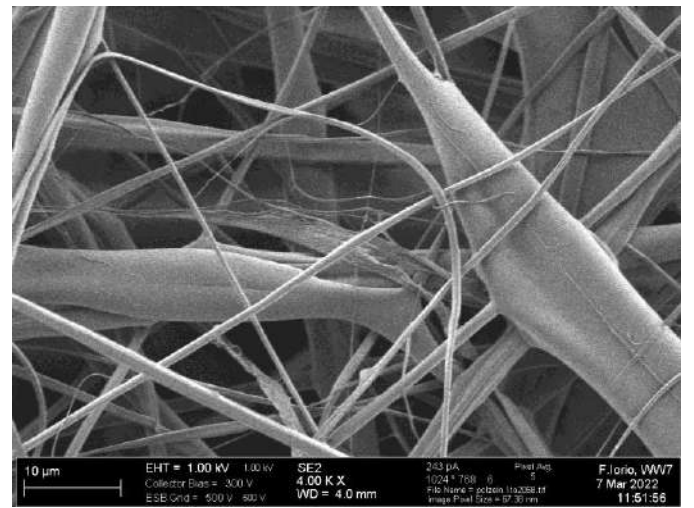
A



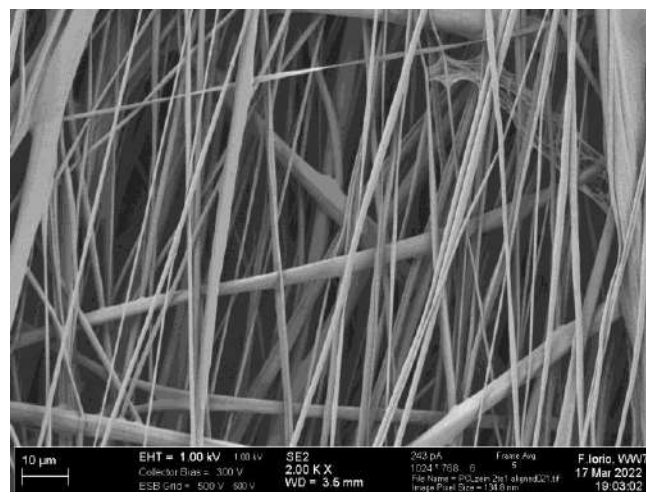
B



C

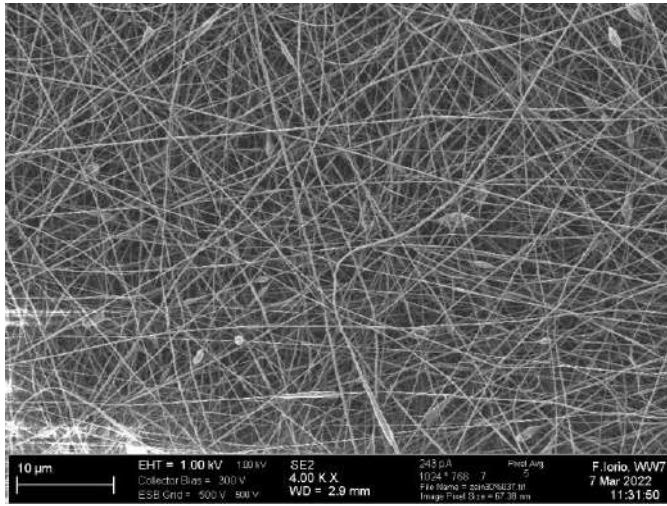


D

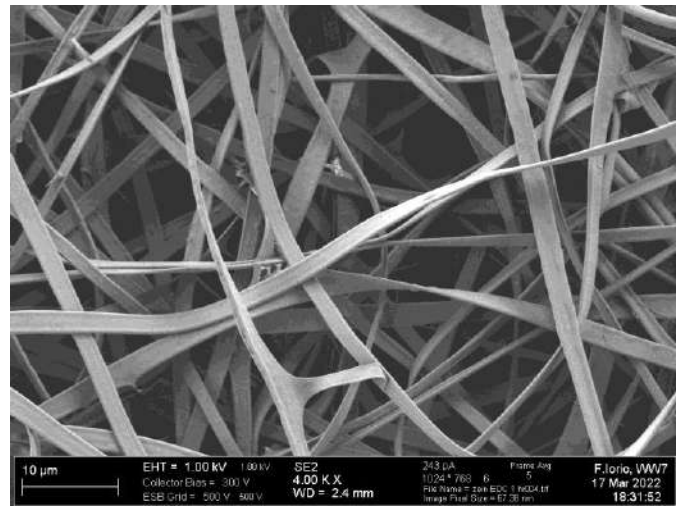


E

Figure 14. SEM images of the samples. (A) PCL 20%. (B) PCL/Zein 2:1 (Random). (C) PCL/Zein 1:1. (D) PCL/Zein 1:2. (E) PCL/Zein 2:1 (Aligned).



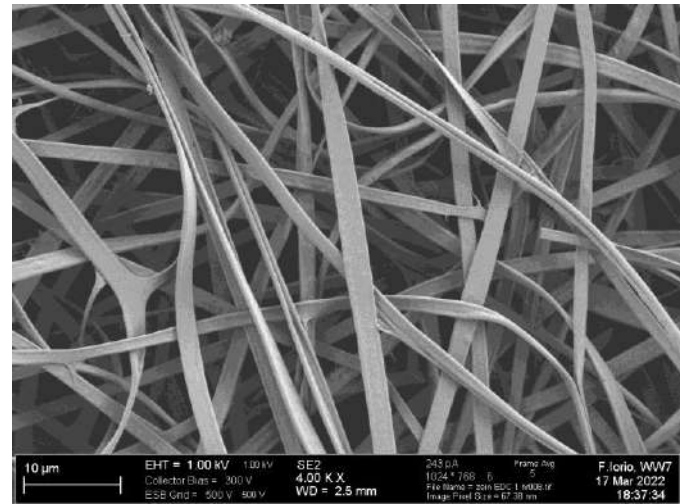
A



B



C



D

Figure 15. SEM micrographs of samples: (A) Zein AA. (B) Zein CC 1 h before spinning. (C) Zein CC 24 h before spinning. (D) Zein CC 72 h before spinning.

Table 2 summarizes the results of these measurements, complemented by the histogram in Figure 16. Additionally, fiber frequency tests are shown in Figure 17.

Sample	Fiber size (μm)
PCL 20%	$0,93 \pm 0,58$
PCL/Zein 2:1	$1,80 \pm 0,79$
PCL/Zein 1:1	$5,19 \pm 2,14$
PCL/Zein 1:2	$2,35 \pm 1,69$
Zein AA	$0,15 \pm 0,05$
Zein CC 1 hs	$2,06 \pm 0,36$
Zein CC 24 hs	$1,94 \pm 0,32$
Zein CC 72 hs	$1,77 \pm 0,36$
Aligned PCL/Zein 2:1	$1,74 \pm 1,62$

Table 2: Average fiber diameter and standard deviation of all samples.

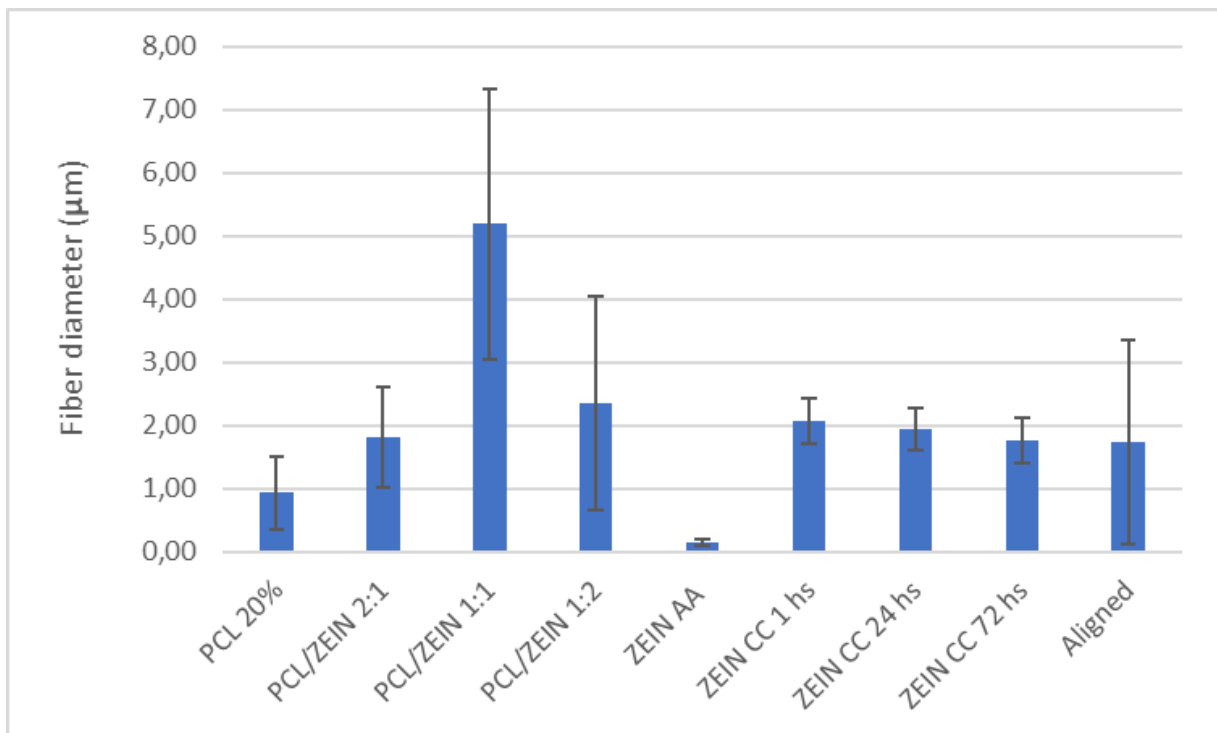


Figure 16: Histogram of the average fiber diameter.

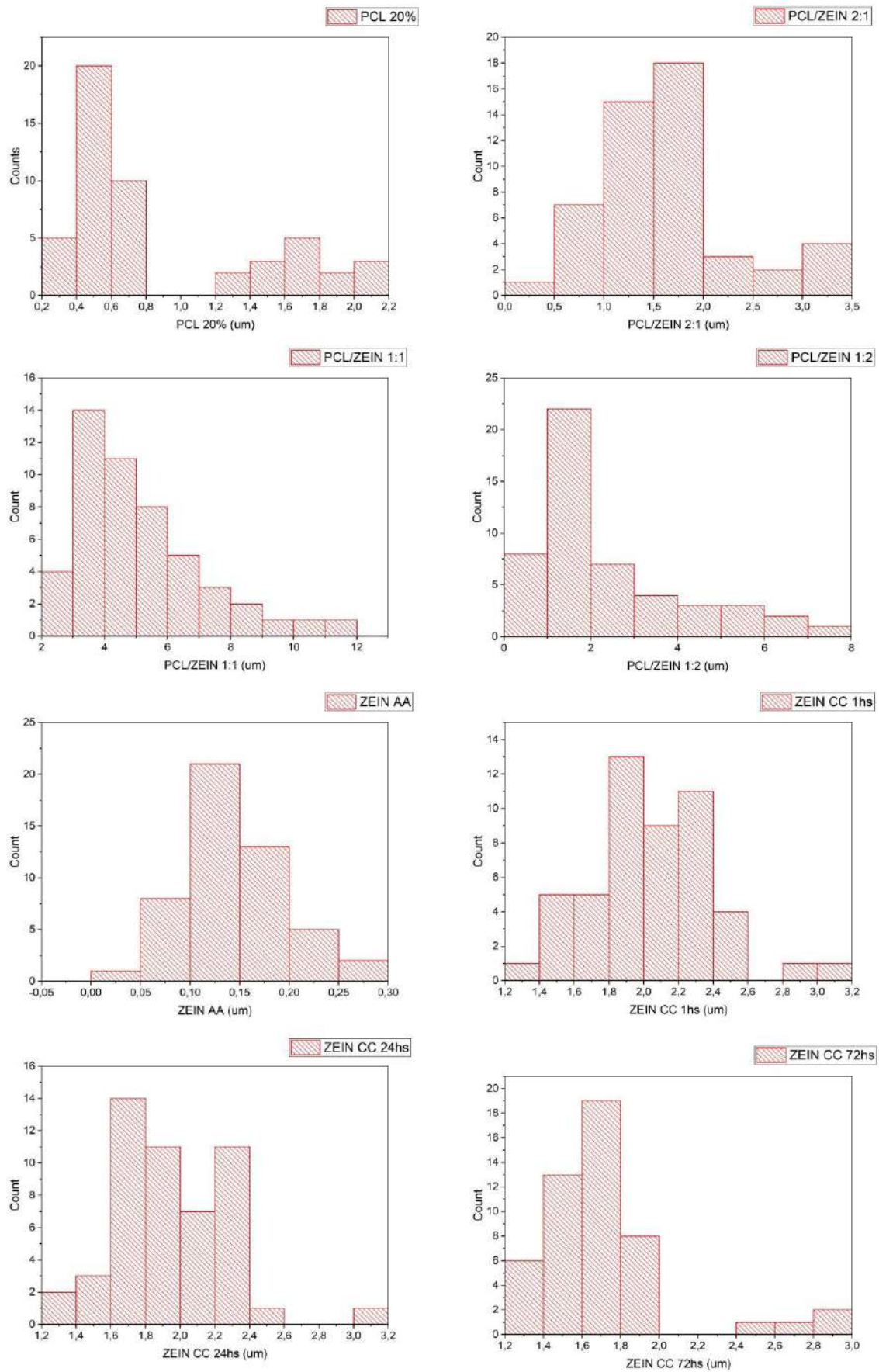


Figure 17: Diameter distribution of all samples

Zein AA displayed the smallest fiber size with an easily identifiable Gaussian distribution. It is followed by the 20% PCL, which exhibited a bimodal size distribution that matches those observed in the SEM micrographs. This implies that the average size is not representative, as it does not capture the size of the majority of the fibers.

Next in terms of size is Zein CC, and it's noteworthy that all sample types (1 hour, 24 hours, and 72 hours) exhibit nearly identical sizes and distribution graphs. This suggests that the various preparation times before electrospinning do not lead to substantial differences

In addition, PCL/ZEIN 2:1 blend, both the random and aligned morphologies, showed similar average sizes but different standard distributions. Upon analyzing the SEM images and the distribution (Figure 18), it appears that there is some form of bimodal distribution, possibly resulting from the fusion of fibers during deposition. This fusing behavior also appears to be replicated in the PCL/ZEIN 1:2 blend. Finally, among the PCL/ZEIN blends, the 1:1 ratio exhibits a substantial difference in the average thickness of the fibers, attributable to their flat morphology.

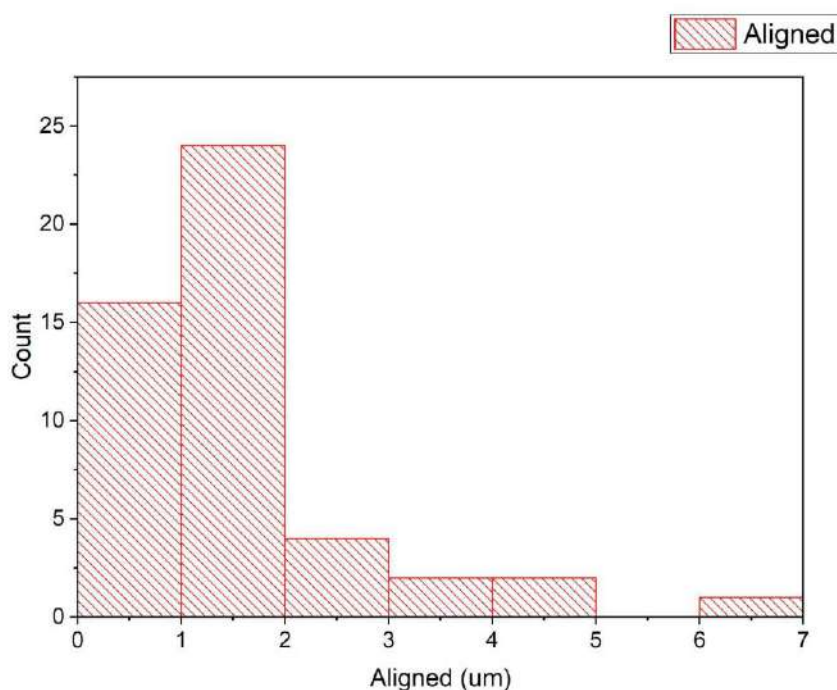


Figure 18 Diameter distribution of PCL/ZEIN 2:1 Aligned

It was also possible to compare the orientation and directionality of fibers in the PCL/ZEIN 2:1 blend. Orientation, measured in degrees, typically refers to the main orientation, which is the direction in which most of the fibers are aligned. However, this information may not always be valuable, as it depends on the specific image and how the sample is positioned in the SEM. Directionality (as opposed to direction) is expressed as a percentage and represents the proportion of fibers aligned along the main direction. This information is significant, as it provides insights into the degree of fiber alignment, which is important when demonstrating the production of aligned fibers compared to random ones.

Finally, by analyzing Figure 19 and 20, the directional graphs for both aligned and randomly oriented fibers were compared. Random fibers, as expected, did not present a preferred angle, and fibers are positioned in all directions. However, when aligned fibers are examined, they exhibit an orientation angle of $83.7^\circ \pm 9.2^\circ$ with a directionality of 65%.

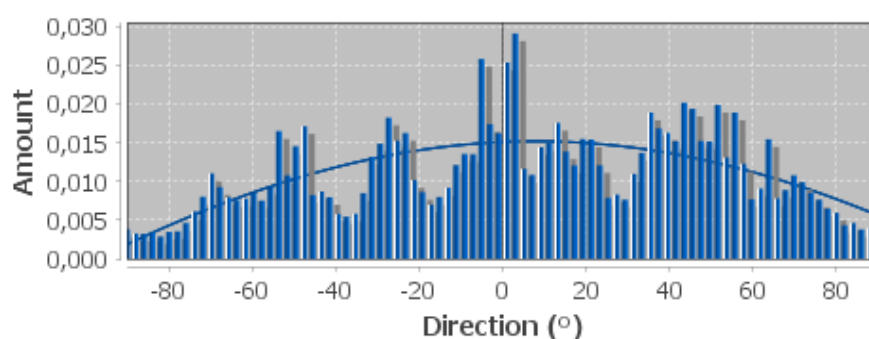


Figure 19: Orientation of the PCL/ZEIN 2:1 fibers (Random)

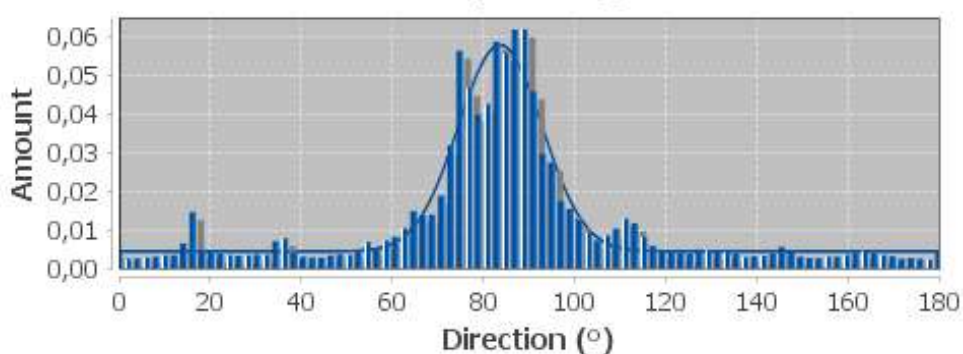


Figure 20: Orientation of the PCL/ZEIN 2:1 fibers (Aligned)

On the other hand, SEM micrographs were used to evaluate the results of the degradation tests carried out on the PCL:ZEIN 2:1 samples. Figure 21 shows SEM micrographs prior to the degradation treatment and one day after exposition to degradation media. There are no changes in the structure because PCL has a long hydrolytic degradation period, even up to 2 years in vitro. However, Zein (AA and CC) by himself degrade in a few days in these conditions. [26].

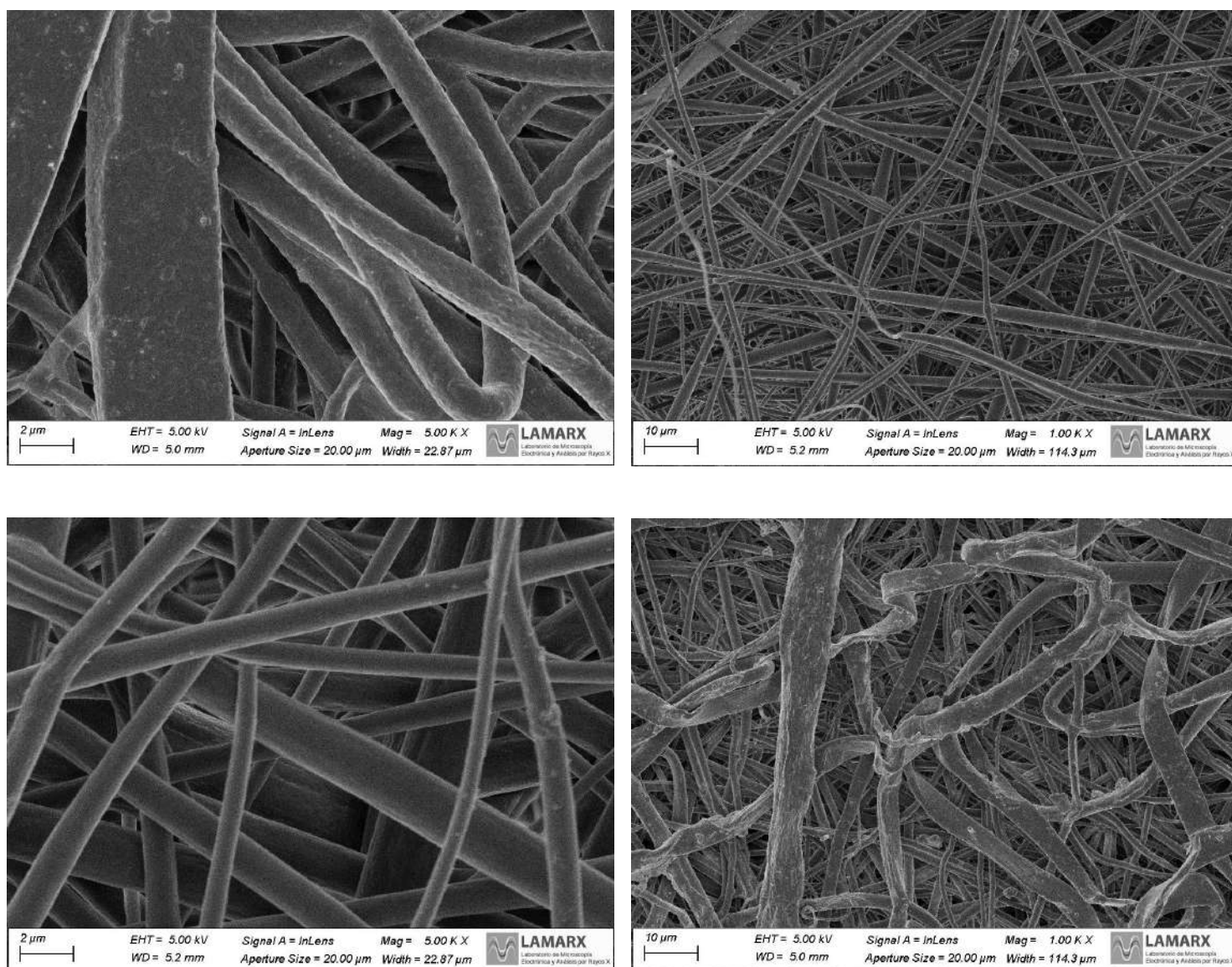


Figure 21: SEM micrograph of PCL/Zein 2:1 before (up) and after (down) degradation test.

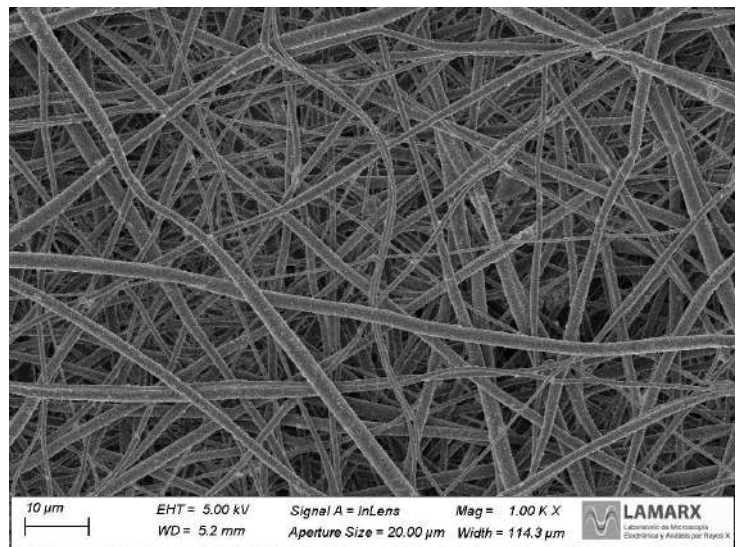
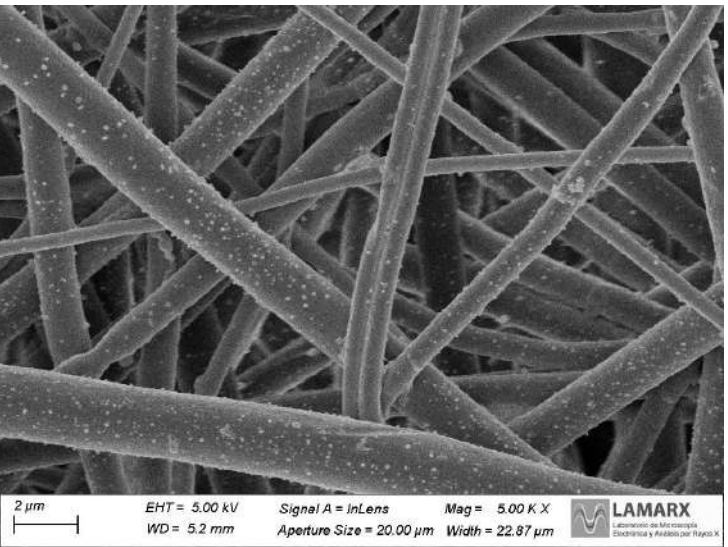
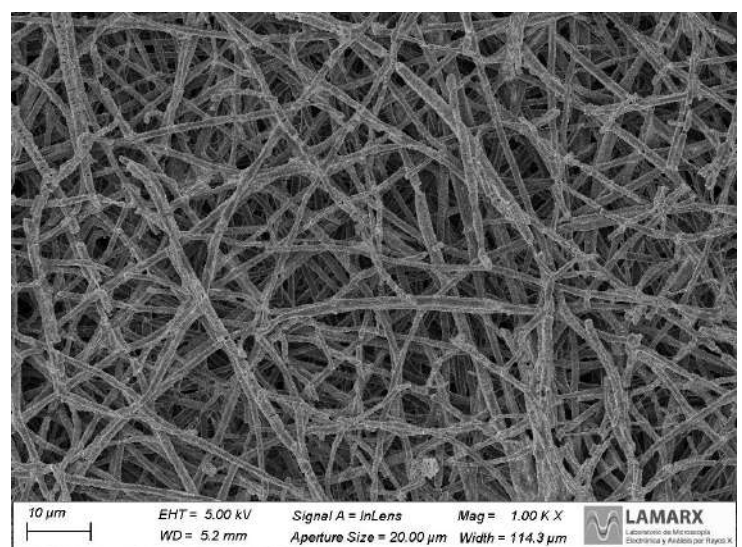
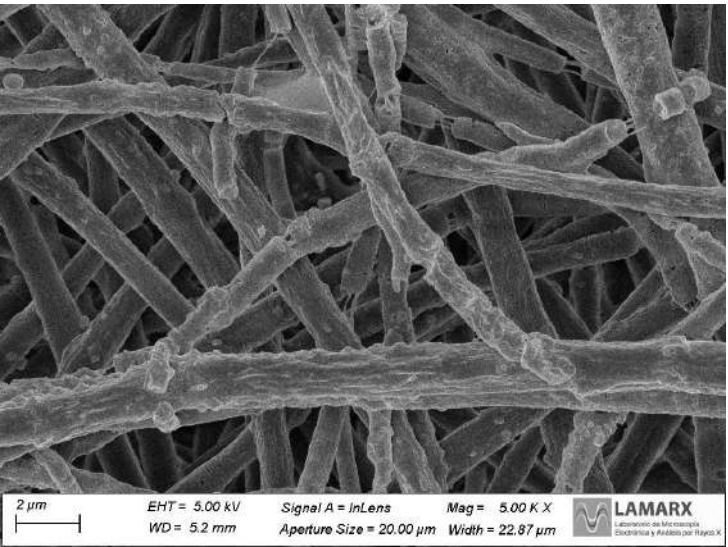
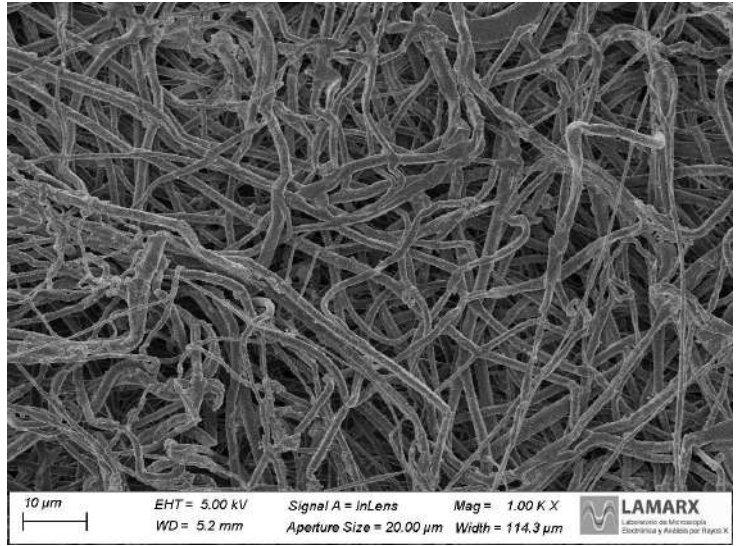
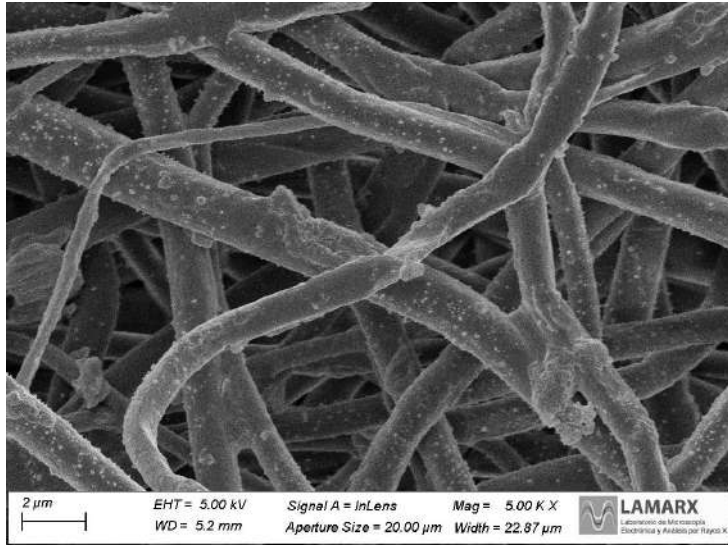


Figure 22: SEM micrograph of PCL/Zein 2:1 after degradation for 7 (up), 14 (center) and 28 (down) days.

After 28 days, some interesting conclusions were obtained (Figure 22). Polycaprolactone (PCL) mixed with zein presented small changes in the degradation behavior. Initial signs of degradation can be observed in the fibers, such as the emergence of dots or beads. This may suggest that zein is coating PCL, causing a certain distortion in the images. However, the general structure at a larger scale remains unchanged at the end of the first month. Even though some fibers, such as the one in Figure 23, may be entirely broken, it is essential to maintain the idea that this is a behavioral trend.

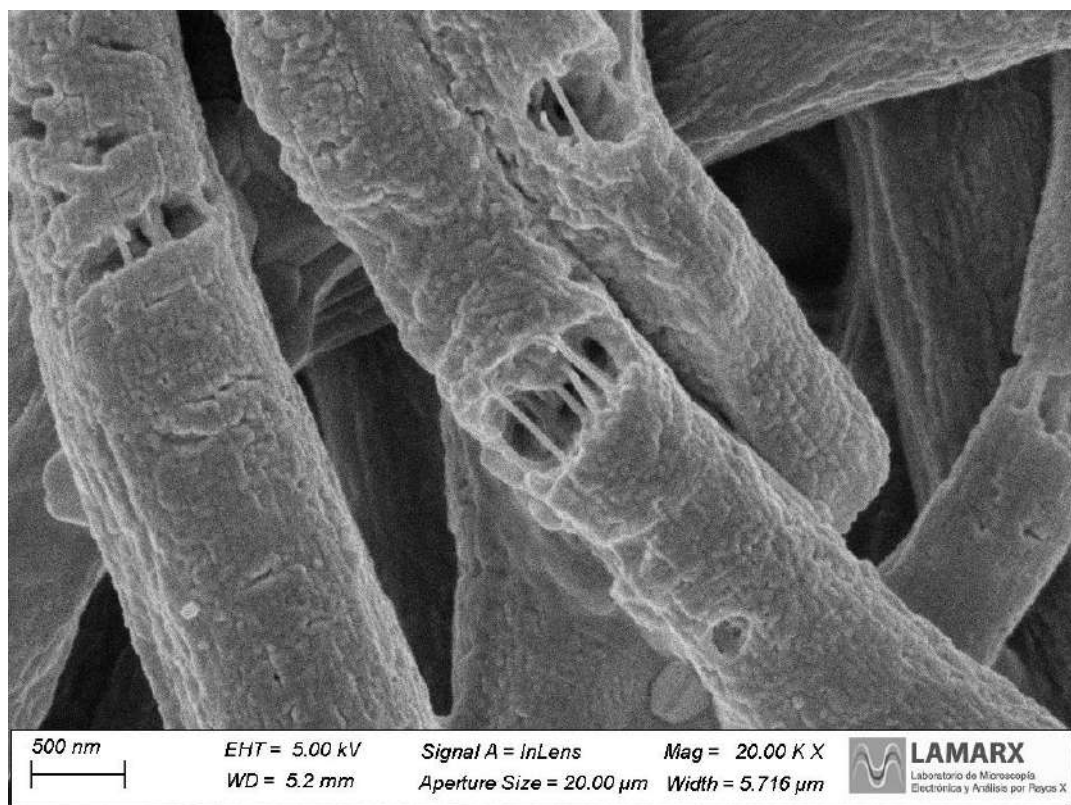


Figure 23: SEM micrograph of PCL/Zein 2:1 after 14 days of degradation.

The average diameter of collagen fibrils ranges from 1-20 μm [4], placing us within the expected size ranges for PCL/ZEIN fibers, as individually these exhibit finer fibers. Additionally, the high degree of directionality achieved in the aligned fibers is ideal for mimicking the organization of collagen fibers in tendon tissue. We have created a biomimetic fibrous scaffold with topographical cues similar to those found in native tendons.

6.2.3 Fourier transform infrared spectroscopy (FTIR)

Knowing that the characteristic peaks of pure zein as reported in the literature are NH group presence at approximately 3300 cm^{-1} , the C-N stretching band around $\sim 1650\text{ cm}^{-1}$, and the C=O stretching band near $\sim 1530\text{ cm}^{-1}$. [22] We will begin by analyzing Zein AA and then compare it with cross-linked Zein.

Figure 24 shows the spectrum of Zein AA. In it, peaks can be observed, detailed in Table 3, indicating the molecule's vibration type. The FTIR spectra reveal the primary vibrational bands of the protein backbone, comprising amide A from 3600 to 3100 cm^{-1} , amine I from 1700 to 1600 cm^{-1} , and amine II between 1600 and 1500 cm^{-1} . The amine I band, sensitive to protein secondary structural components, represents the C=O stretching vibration. Conversely, the amine II band arises from N-H bending and C-N stretching vibrations [23].

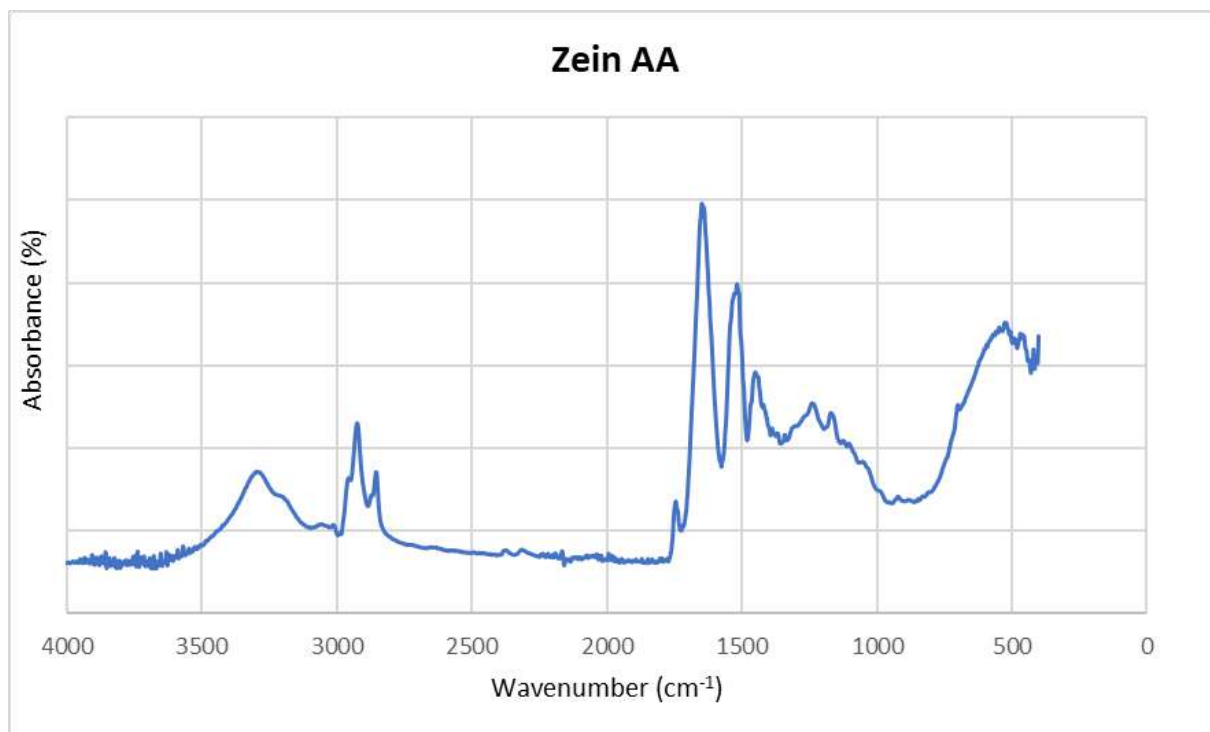


Figure 24: FTIR spectrum for ZEIN AA

Wavenumber (cm ⁻¹)	Functional Group	Type of Vibration
3300	N - H	Stretching
1650	N - O	Stretching
1530	C = O	Stretching

Table 3: FTIR peaks for Zein AA

Following the comparison line, we proceed with Zein CC, as shown in Figure 25 and Table 4. As expected, since we are dealing with the same material, the same groups are present. However, it would be expected that the cross linked groups have larger peaks (usually amine bands I and II) than those of Zein AA. Additionally, no significant differences are observed among the three types of Zein CC samples (also expected).

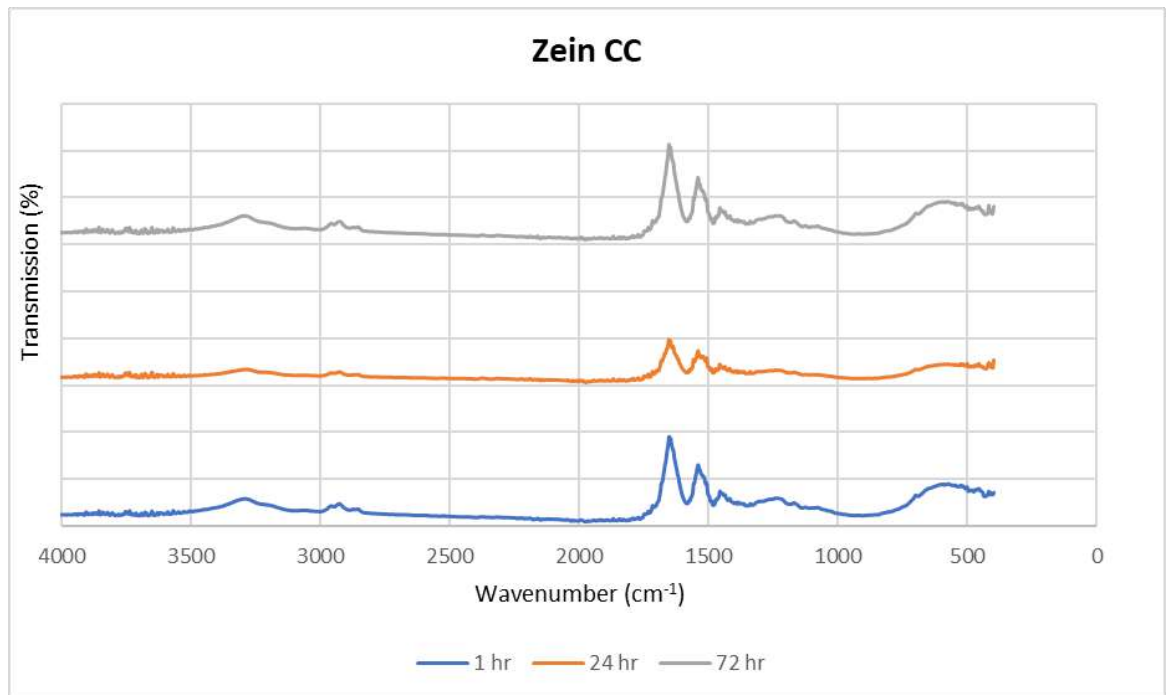


Figure 25: FTIR spectra for ZEIN CC at 1 h, 24 h and 72 h prep. before spinning

Wavenumber (cm ⁻¹)	Functional Group	Type of Vibration
3300	N - H	Stretching
1650	N - O	Stretching
1530	C = O	Stretching

Table 4: FTIR main bands assignment for Zein CC

Continuing with the procedure, we will now analyze the spectrum of PCL 20%, as depicted in Figure 26. As it is well known, the characteristic band of PCL appears at around $\sim 1720\text{ cm}^{-1}$, corresponding to the C=O stretching of the ester carbonyl group. Additionally, C-H asymmetric and symmetric stretching can be identified at 2940 and 2862 cm^{-1} , respectively [24]. As shown in Table 5, these peaks align with those observed in the analyzed sample.

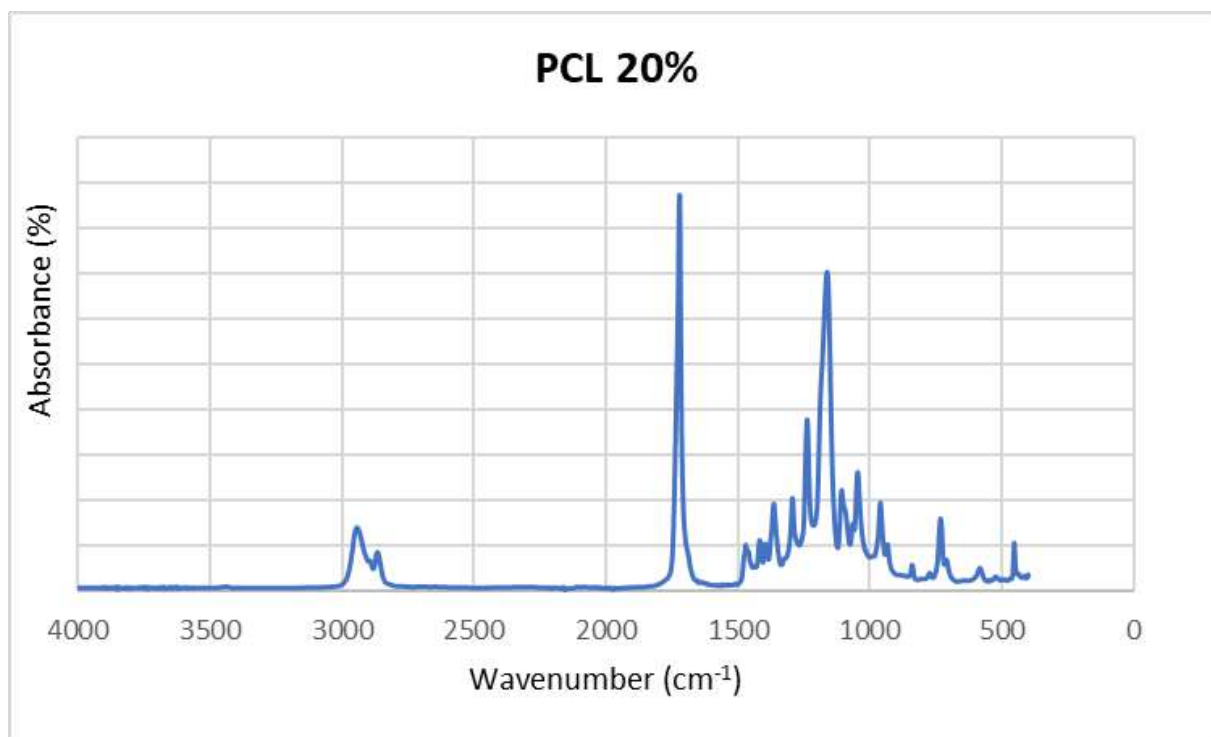


Figure 26: FTIR spectrum for PCL 20%

Wavenumber (cm ⁻¹)	Functional Group	Type of Vibration
2950	C - H	Asymmetric stretching
2865	C - H	Symmetric stretching
1720	C = O	Stretching

Table 5: FTIR main bands assignment for PCL 20%

As expected, the theoretical values of PCL in the literature coincide with those observed in the analyzed samples [24]. Finally, we will proceed to analyze FTIR spectra for the different blends of PCL/Zein at their various ratios as can be seen in figure 27. The present groups have 3 samples each (m1, m2 and m3) and their respective assignments can be seen in Table 5.

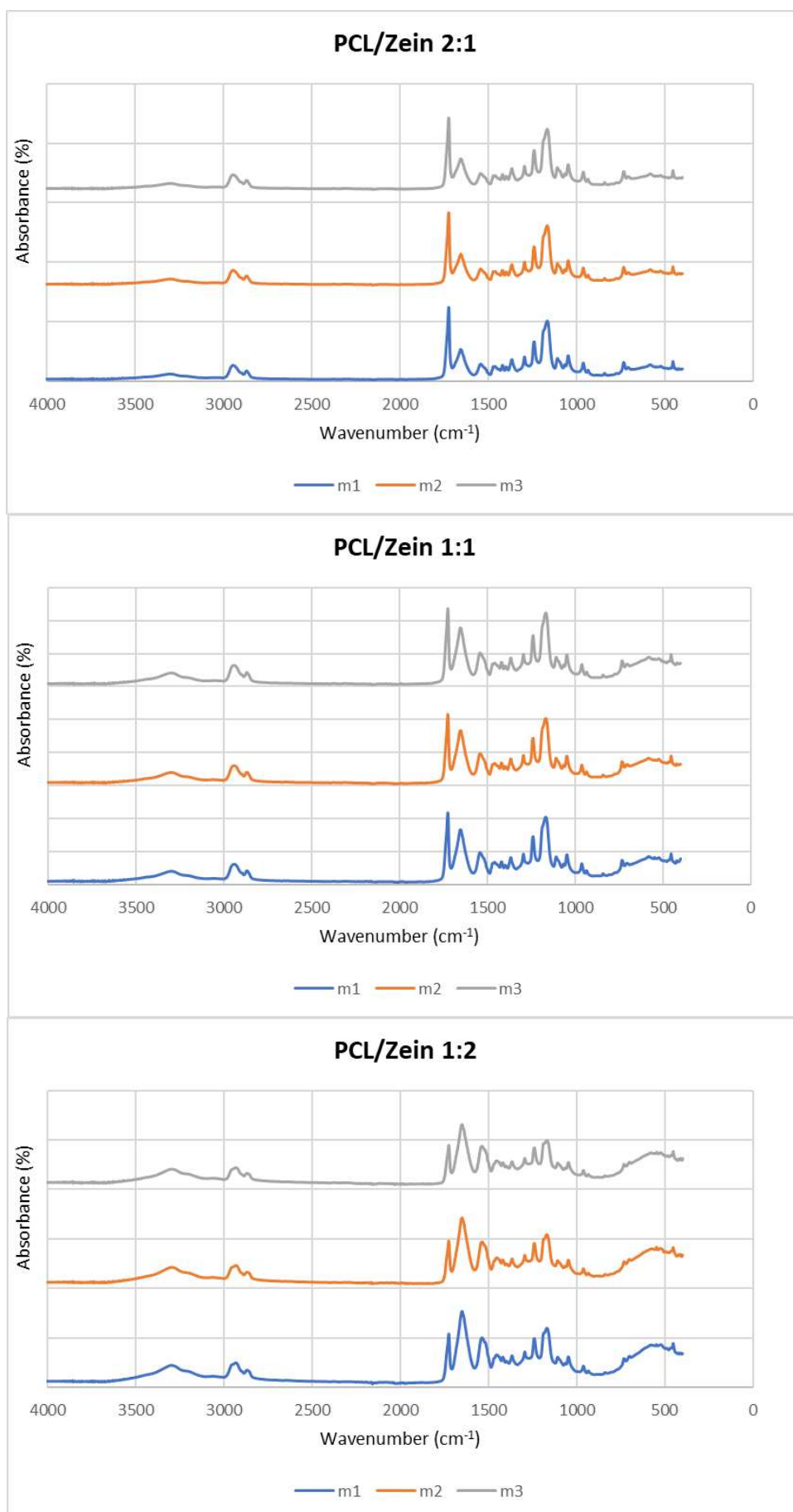


Figure 27: FTIR spectra for PCL/ZEIN at 2:1, 1:1 and 1:2 ratios.

Wavenumber (cm ⁻¹)	Functional Group	Type of Vibration	
3300	N - H	Stretching	Zein
2950	C - H	Asymmetric stretching	PCL
2865	C - H	Symmetric stretching	PCL
1720	C = O	Stretching	PCL
1650	N - O	Stretching	Zein
1530	C = O	Stretching	Zein

Table 6: FTIR main bands assignment for PCL/ZEIN blends

As seen in the blends, the functional groups of both PCL and Zein are present, indicating that both are retained after electrospinning. Additionally, as expected, there are no differences between their spectra despite having different material proportions.

Finally, once the decision was made to manufacture aligned fibers with a blend of PCL/ZEIN 2:1, FTIR spectra were acquired again from the samples. This resulted in the spectra shown in Figure 28 and the peaks are the same as can be seen in table 6.

The results for PCL/ZEIN 2:1 random and aligned are the same, as expected since they both come from the same chemical structure. In the literature, it's observed that the FTIR of fibers created from the same material but with different orientation show no changes [25]. Thus, we can conclude that the FTIR results are not affected by the orientation of the fibers.

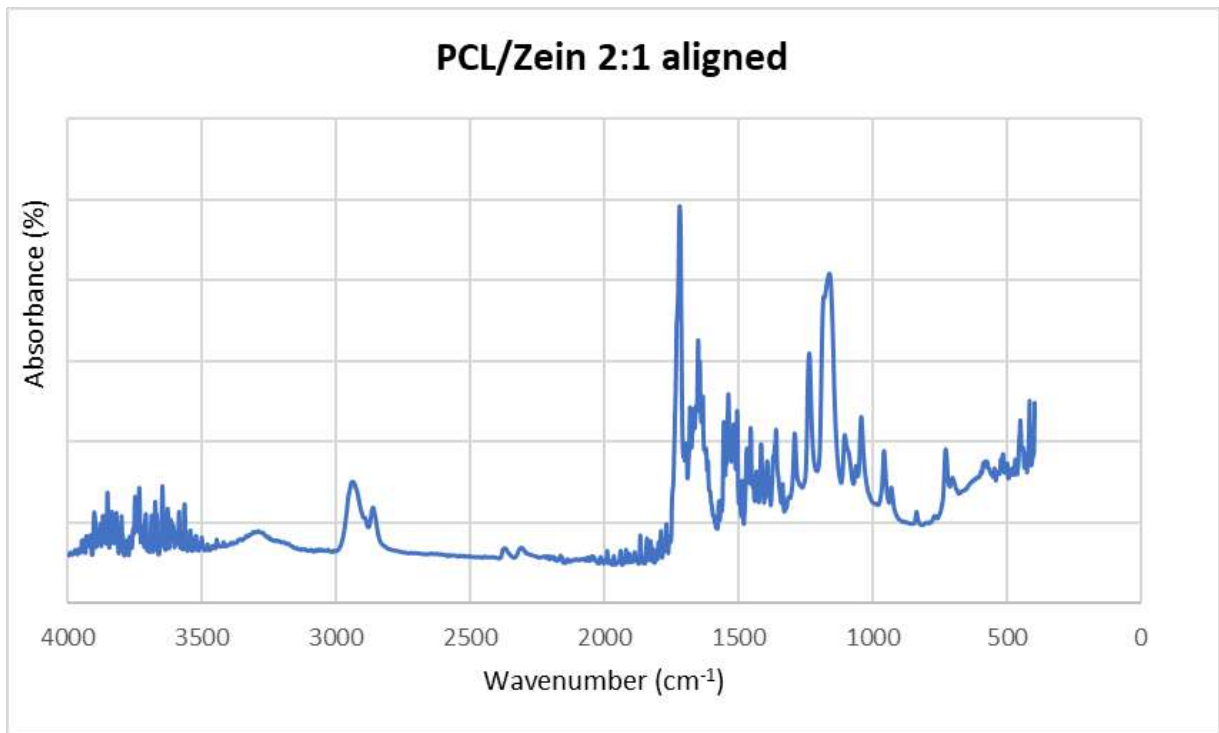


Figure 28: *FTIR spectra for PCL/ZEIN 2:1 Aligned*

6.2.4 Mechanical tests

Regarding mechanical testing, it is crucial to understand that the results do not reflect a specific mechanical property of the materials. This is because the tested samples comprised randomly oriented fibers. Consequently, the acquired values characterize the nanofibrous matrix as a complete entity rather than any individual fiber.

Mechanical tests were conducted on all the produced fibers: PCL 20%, PCL/Zein 2:1 (random and aligned), PCL/Zein 1:1, PCL/Zein 1:2, and Zein AA. The only exception was with the Zein CC samples, as they were extremely fragile and couldn't be handled. When placing these fibers on the charge cells, they were impossible to detach from the aluminum film, resulting in the test providing data corresponding to an aluminum film rather than the fiber. This can be observed in Figure 29.

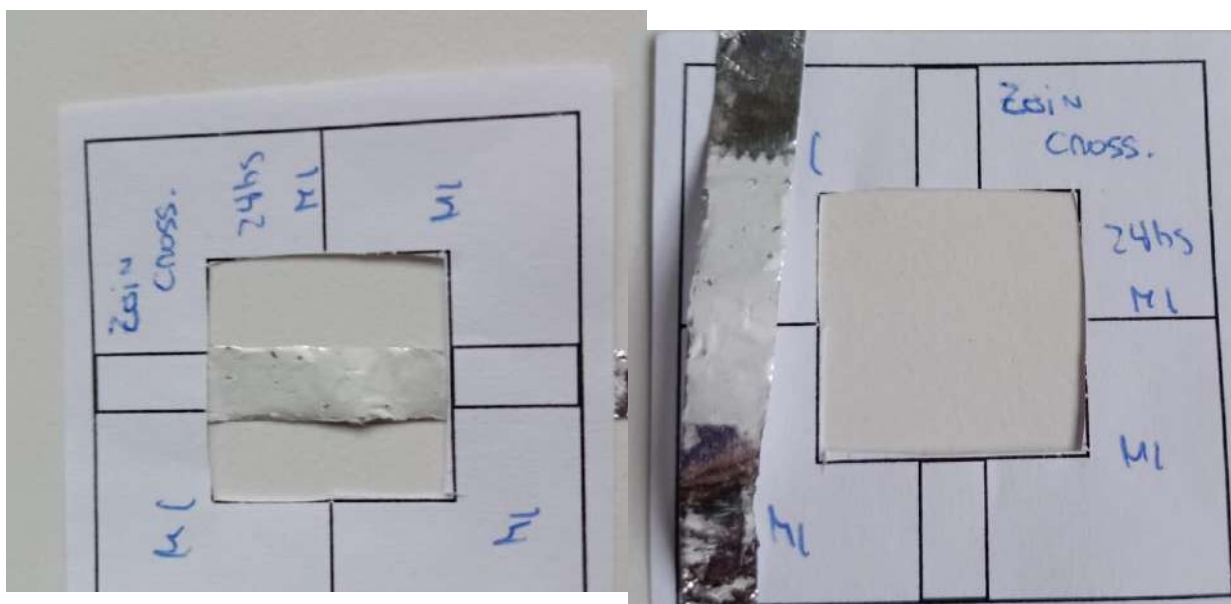


Figure 29: *Difficulties in carrying out mechanical tests on Zein CC*

Afterward, 3 experiments were conducted on Zein AA (m1, m2 m3). The samples withstood the necessary handling to place them in the cells, carrying out three trials, as depicted in Figure 30. The results yielded a Young's modulus close to (23.6 ± 11.7) MPa and Stress at Break of (0.45 ± 0.1) , and the graphs of the three samples are shown in Figure 31.

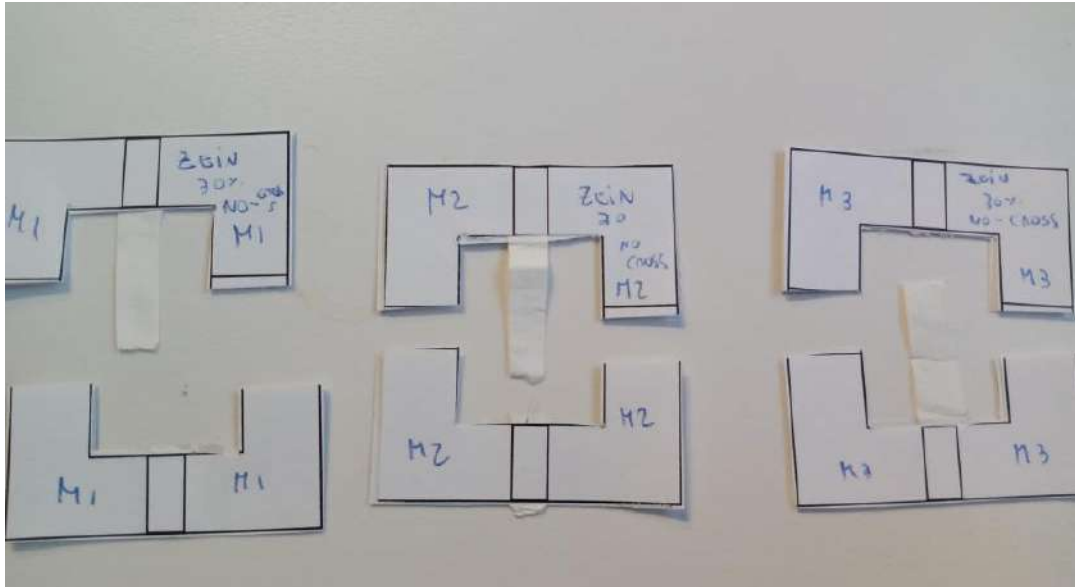


Figure 30: Zein AA samples after tensile tests

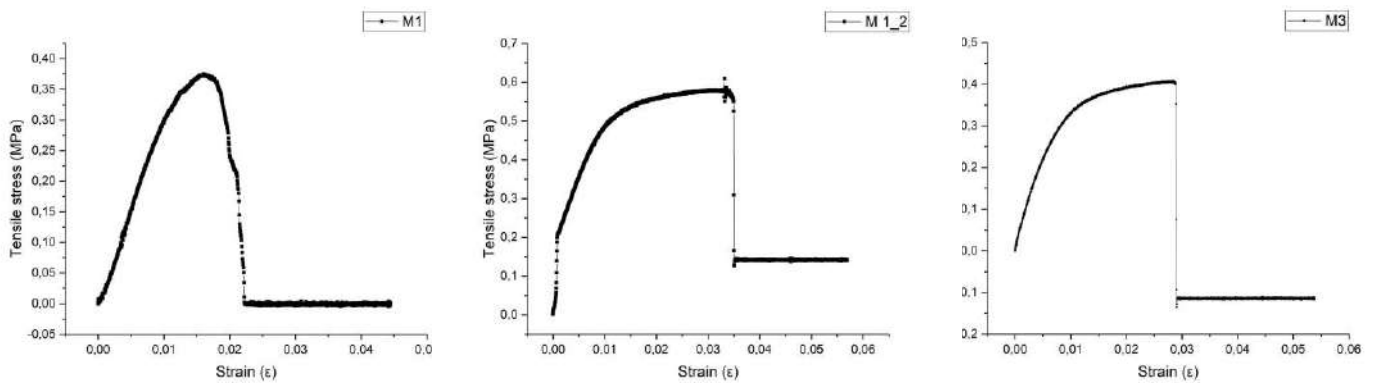


Figure 31: Stress vs strain curves of Zein AA

Next, tests were conducted on PCL at 20%, as illustrated in Figure 32. Sample 1 exhibited a significantly higher elongation at break than the other two (Figure 32 A). As mentioned earlier, this serves as a reminder that the results represent a trend, as they depend on factors such as the orientation of the fiber mats being analyzed, local thickness of the mat depending on how the fibers are deposited on the collector, etc. This variation is further evident in the comparison of stress-strain curves on Figure 32 (B). Nevertheless, the stiffness determined by Young's modulus was very similar in all three samples, averaging (38.5 ± 3.1) MPa and a stress at break of (2.46 ± 0.1) MPa. Comparing Zein AA and PCL 20%, significantly higher elongation at break and greater stiffness are evident in the synthetic polymer fiber mats.

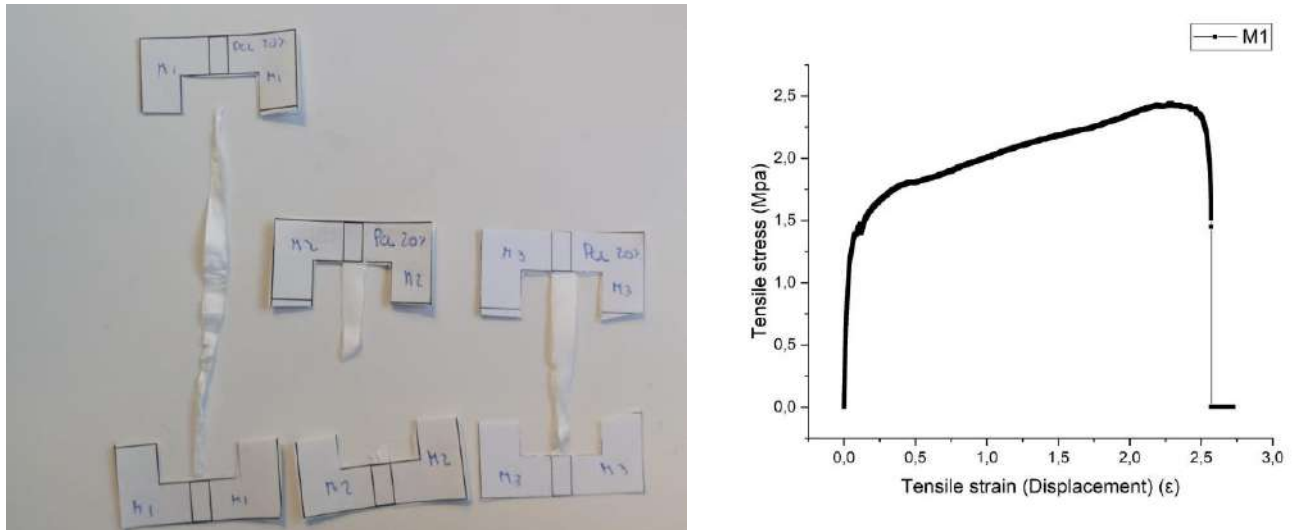


Figure 32: (A) PCL 20% Samples after tensile test. **(B)** Strain vs stress curve of PCL 20% Sample 1.

Subsequently, tests were conducted on the blends of PCL/ZEIN fibers, starting with the PCL/ZEIN 2:1 fibers with random orientation. The samples are depicted in Figure 33. At first glance, it is evident that the stiffness and the elongation at break was greater than in the Zein AA samples, this is supported by the stress-strain curves shown in Figure 34. In these curves, an elongation at break almost ten times higher than that observed in pure Zein is evident. Additionally, the average Young's modulus is (129.6 ± 10.1) MPa, significantly higher than that of pure PCL and Zein. This is a good result because healthy human tendons Young Modulus are around 100-1000 MPa [28] On the other hand, the stress at break is (2.39 ± 0.1) MPa, slightly lower than that of pure PCL but several times higher than that of Zein.

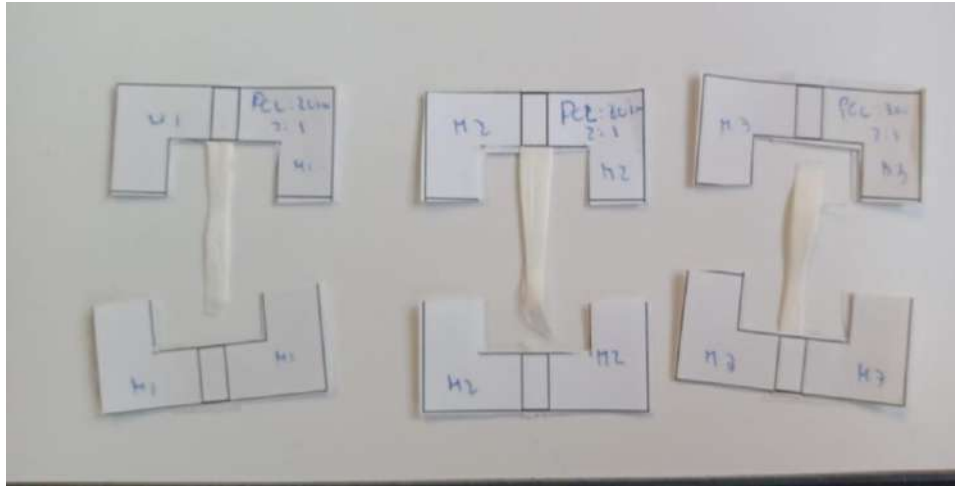


Figure 33: PCL/ZEIN 2:1 samples after tensile test

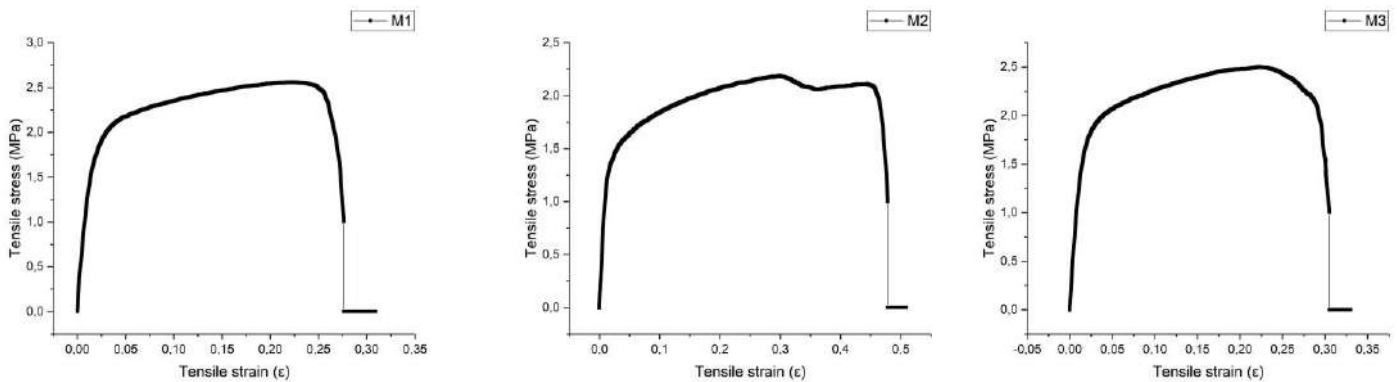


Figure 34: Stress vs Strain curves of PCL/ZEIN 2:1 Random

Subsequently, tests were conducted on the PCL/ZEIN 1:1 blend. In Figure 35, the results of the four conducted samples are presented, as one of the results had to be discarded. Additionally, a peculiar observation was made as the samples appeared to be composed of layers of fibers, as depicted in Figure 29. This suggests the possibility of a certain fragility, as instead of forming a mat of fibers with certain thickness, the samples might be prone to delamination.

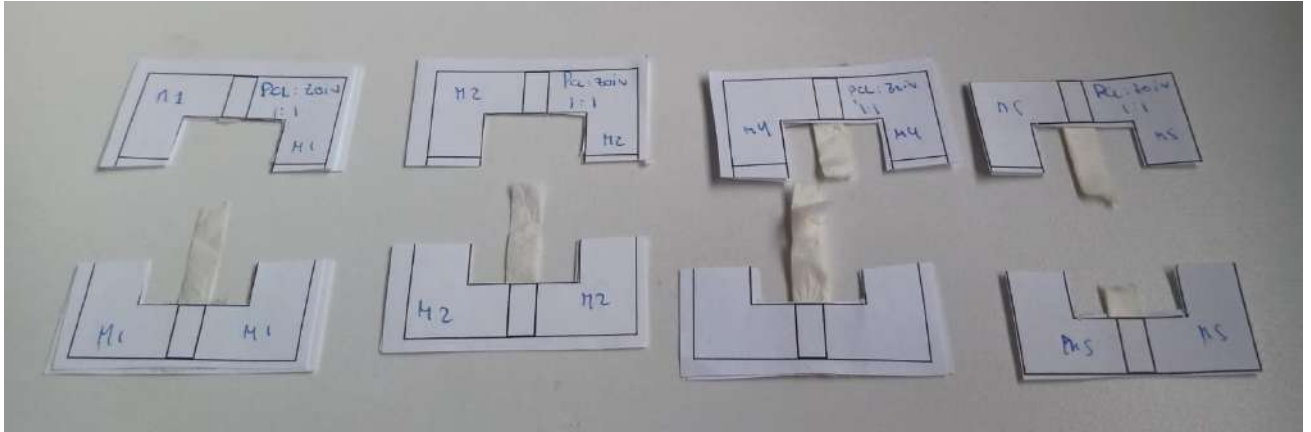


Figure 35: *PCL/ZEIN 1:1 samples after tensile test*

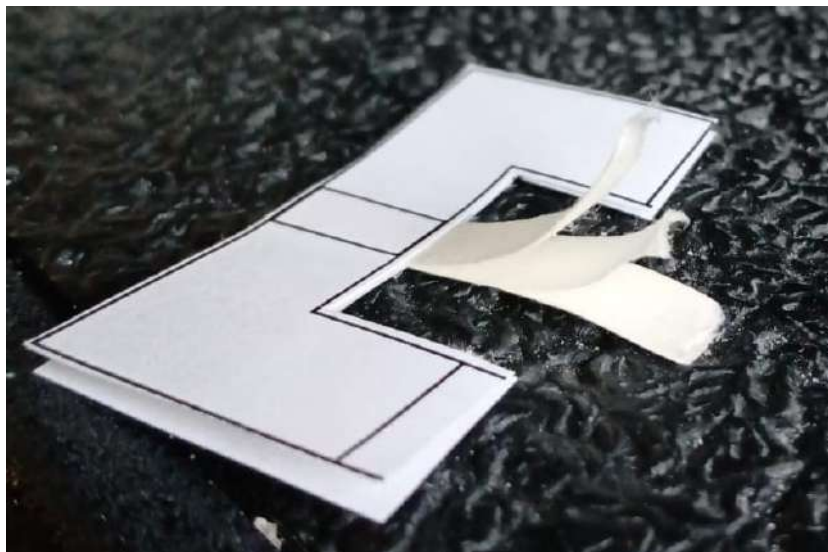


Figure 36: *Image of PCL/ZEIN 1:1 sample showing delamination events*

When analyzing the stress-strain curves of the samples (Figure 37), interesting conclusions can be drawn. Stress at Break (0.49 ± 0.1) MPa and the elongation at

break decreases again to levels comparable to those of Zein AA. Young's modulus yields a result of (49.8 ± 15.6) MPa, giving better stiffness than the PCL and ZEIN., One could speculate that a higher proportion of Zein may lead to a reduction in properties compared to the other blend with a 2:1 ratio.

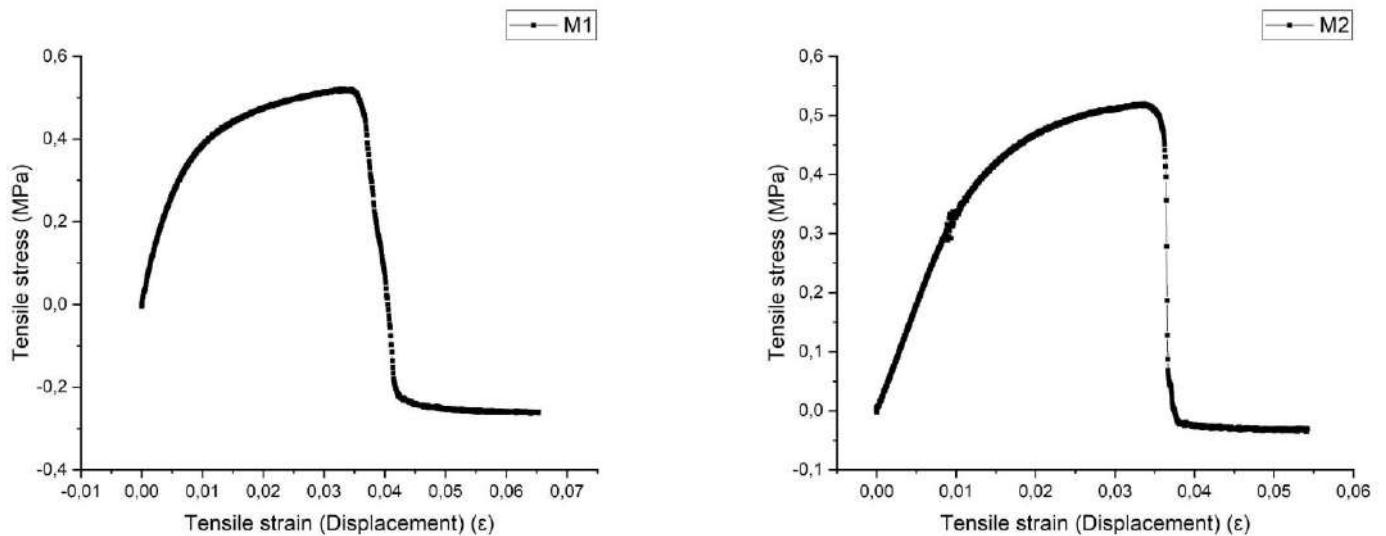


Figure 37: *Stress vs Strain curves of PCL/ZEIN 1:1*

Finally, the last blend tested was the PCL/ZEIN 1:2 (Figure 38). No particularities were observed during the testing, and Young's modulus was (31.3 ± 10.1) MPa, closer to the values of Zein AA. Additionally, as seen in the curves (figure 39), it exhibits a low elongation and stress at break. (0.22 ± 0.1) MPa, worse properties compared to the other blends. This could be attributed to the higher proportion of Zein in its composition, or even consider that the parameters were not optimized. As it was also possible to see in the SEM images, a kind of bimodal structure with non-uniform fiber sizes could give us indications of this.

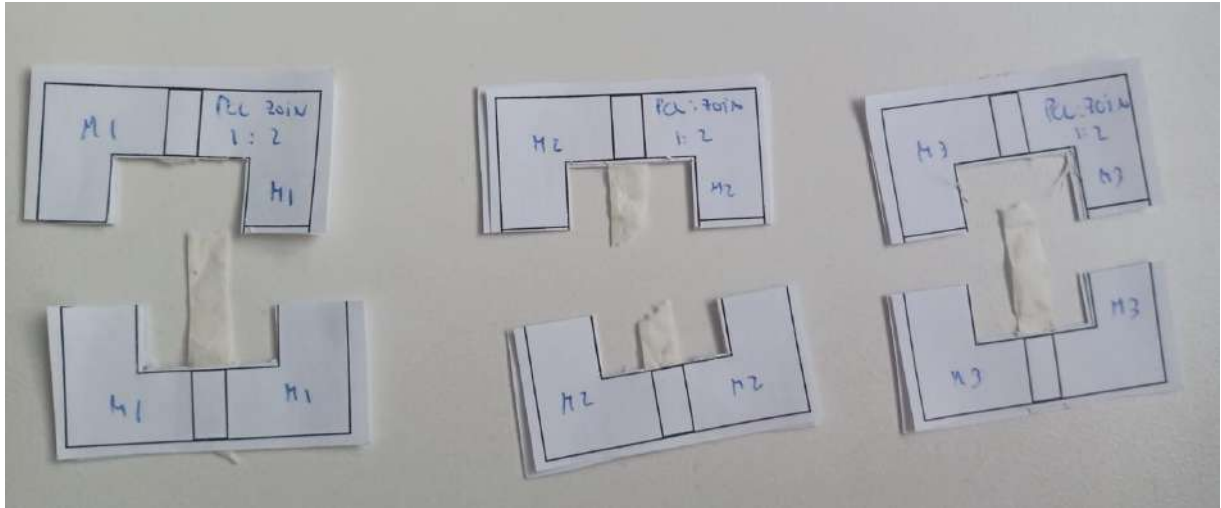


Figure 38: PCL/ZEIN 1:2 samples after tensile tests

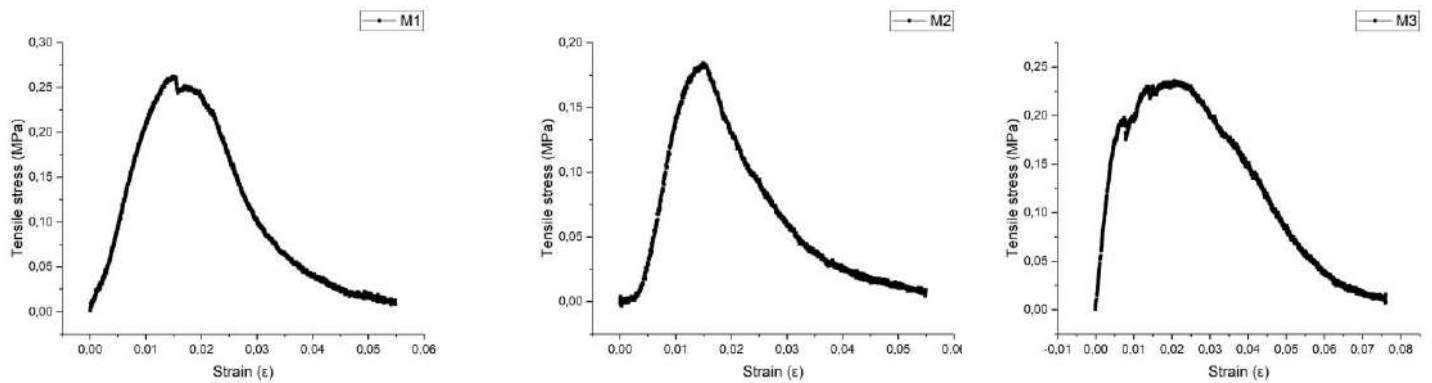


Figure 39: Stress vs Strain curves PCL/ZEIN 1:2

Based on observations from SEM images and mechanical tests, significant progress was achieved in producing aligned fibers from the PCL/ZEIN 2:1 blend. In the mechanical tests (see Figure 40), higher tensile strength, stress, and elongation at break were evident compared to fibers with random orientation. Moreover, Young's modulus nearly doubled, reaching values of (301.3 ± 18.1) MPa [27]. These findings

are consistent with the organization of the fibers, as the tendency for alignment significantly enhances mechanical properties.

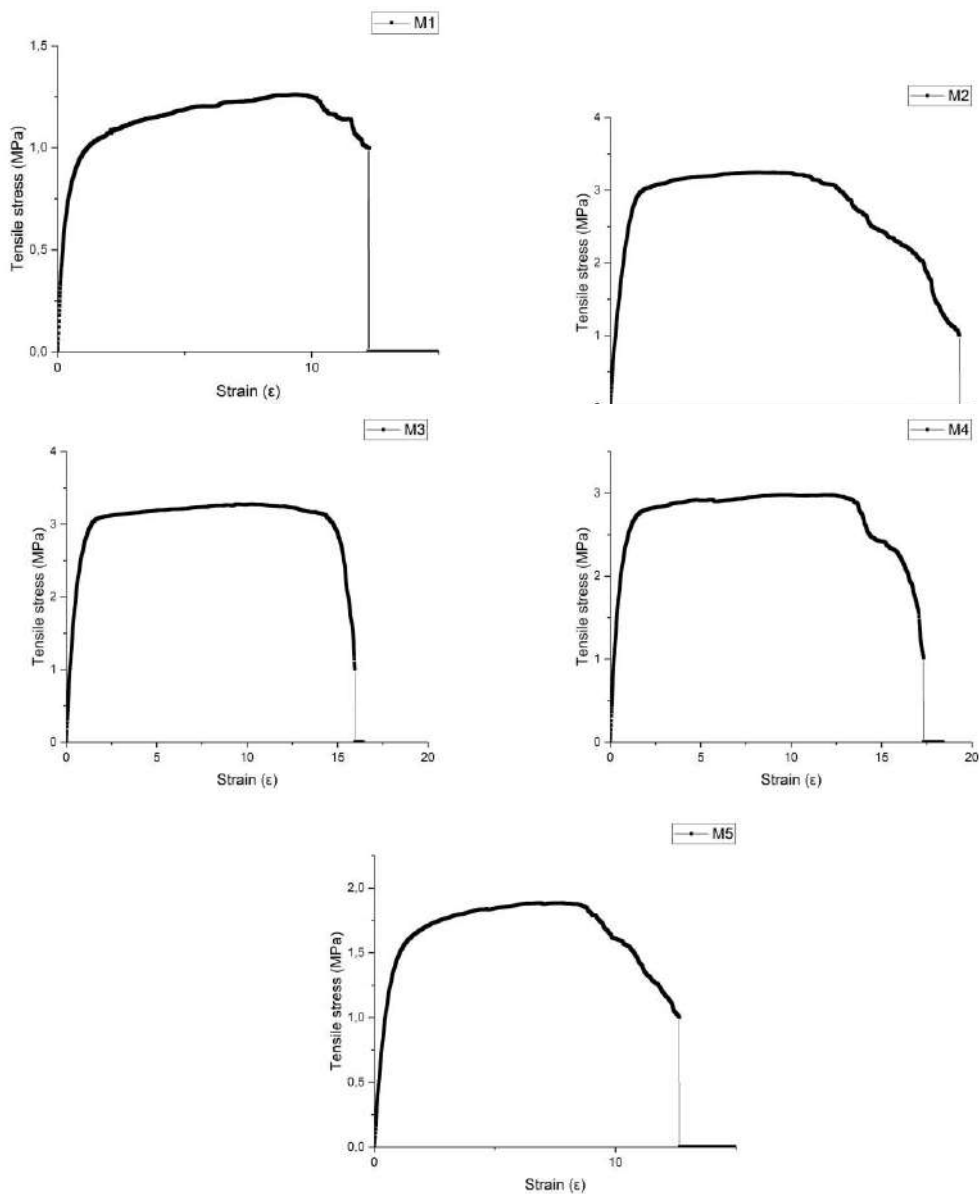


Figure 40: Stress vs strain curves PCL/ZEIN 2:1 with aligned nanofibers

Table 7 summarizes all the results of Young's modulus and breaking stress of the different samples.

	Young Modulus (MPa)	Stress at Break (MPa)
Zein AA	(23.6 ± 11.7)	(0.45 ± 0.1)
PCL 20%	(38.1 ± 11.7)	(2.46 ± 0.1)
PCL/ZEIN 2:1 (Random)	(129.6 ± 10.1)	(2.39 ± 0.2)
PCL/ZEIN 1:1	(49.8 ± 15.6)	(0.49 ± 0.1)
PCL/ZEIN 1:2	(31.3 ± 10.1)	(0.22 ± 0.1)
PCL/ZEIN 2:1 (Aligned)	(301.3 ± 18.1)	(2.80 ± 0.7)

Table 7: *Tendency of the mechanical properties of all the samples*

Finally, it is evident that the mechanical properties of the PCL/ZEIN blend either matched or surpassed those exhibited by the 20% PCL alone, fulfilling the primary objective of these blends. Additionally, the alignment of fibers further enhanced these properties, bringing them closer to the desired characteristics sought in tendon tissue engineering.

We cannot disregard the fact that only three tensile tests were conducted for each sample in an attempt to determine the most optimal for subsequent testing. To draw more robust conclusions and establish trends, a viable option would be to conduct a minimum of 10 tests per sample. Unfortunately, this was not feasible due to the diverse array of fibers, which would have required a significant amount of time to manufacture a sufficient quantity of samples and conduct the tests.

6.2.5 Contact angle measurements

Wettability of a polymer surface is one key factor to influence cell–material interaction and the subsequent cell behaviors. This depends on surface functional groups, structure, the surface roughness of the material among other parameters. Wettability can control essential protein adsorption on the polymer surface and subsequently affect cell activities [29].

Five measurements were conducted for each type of sample under analysis. The individual measurements for PCL and Zein were as expected, given their hydrophobic and hydrophilic nature, respectively. As shown in Figure 41A, after 10 seconds, the contact angle of PCL is $102.24 \pm 3.02^\circ$. In contrast, Zein completely penetrates through the porous structure, disappearing entirely from the surface before reaching 10 seconds.

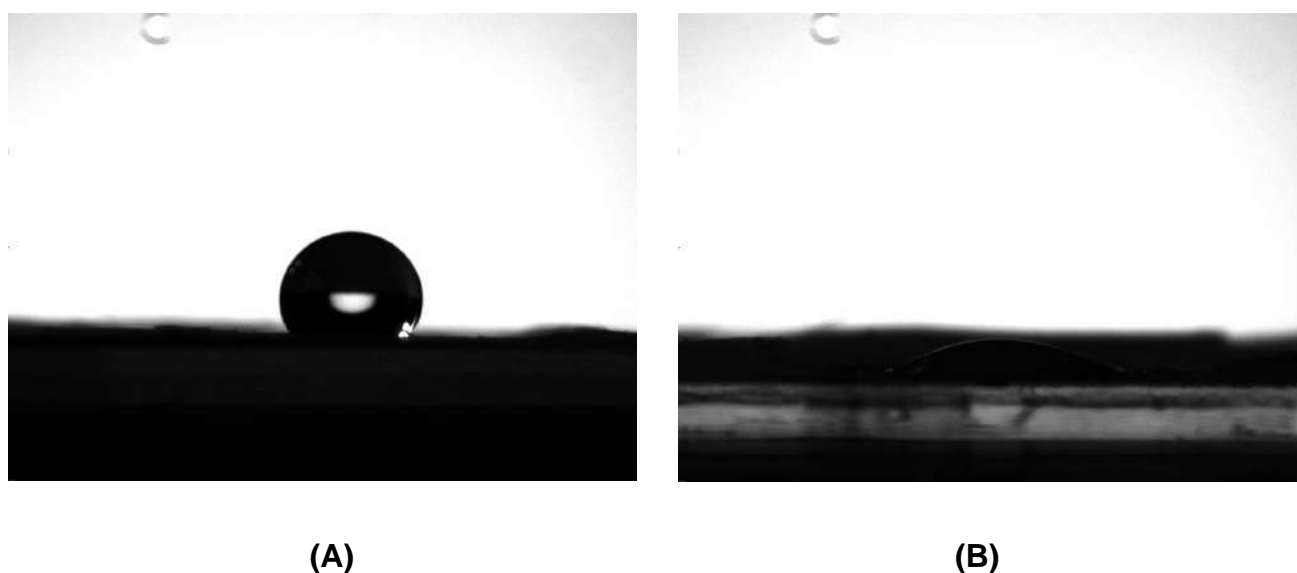


Figure 41: *Water drops in contact angle measurements at 10 seconds for samples: (A) PCL 20%. (B) Zein 30%.*

Continuing with Zein CC in all its variants (1 h, 24 h, 72 h), the results were consistent with those observed in Zein AA (Figure 42). After 10 seconds, all droplets completely permeate the structure, suggesting that crosslinking does not alter the hydrophilicity of Zein. Additionally, as observed in the SEM images, the porous structure continues to play a key role in the permeability of the samples.



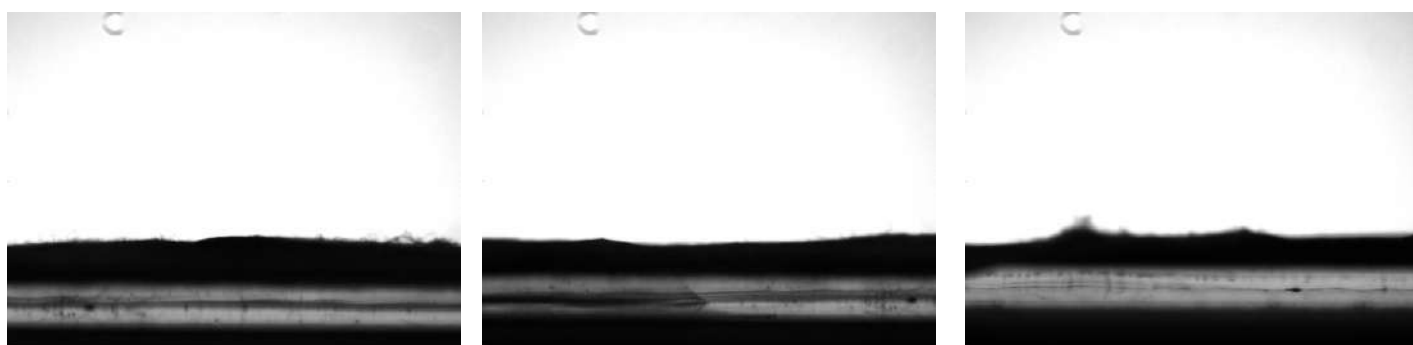
A

B

C

Figure 42: *Water drops in contact angle measurements at 10 seconds for Zein CC samples: (A) 1 h, (B) 24 h, (C) 72 h*

The same results were observed in the PCL/ZEIN blends (Figure 43: A 2:1, B 1:1, and C 1:2). The water droplets penetrated their structure after a few seconds, suggesting superhydrophilic behavior. Typically, most animal cells prefer a surface with moderate hydrophilicity for adhesion and growth. Surfaces that are either superhydrophilic or superhydrophobic are generally unfavorable for cell attachment and growth. However, in this case, it was found that the more hydrophilic the polymer surface, the more fibroblasts adhere and spread widely, resulting in good adhesion, as demonstrated in the cell viability test [29].



A

B

C

Figure 43: *Water drops in contact angle measurements at 10 seconds for PCL/ZEIN samples: (A) 2:1, (B) 1:1, (C) 1:2*

6.2.6 Degradation Test

Degradation tests were conducted on the PCL/ZEIN 2:1 samples. First, the water uptake of the samples was analyzed, as it is an important parameter that reflects their behavior towards water diffusion and absorption. These parameters are crucial to ensure cell growth and proliferation as they guarantee nutrition and blood supply within the samples.

As can be seen in the graphs (Figure 44), water absorption is quite high and shows a slight tendency to increase over the days. However, the data dispersion may be attributed to the low mass of the samples, where small variations in thickness, environmental conditions, or even handling can lead to these results.

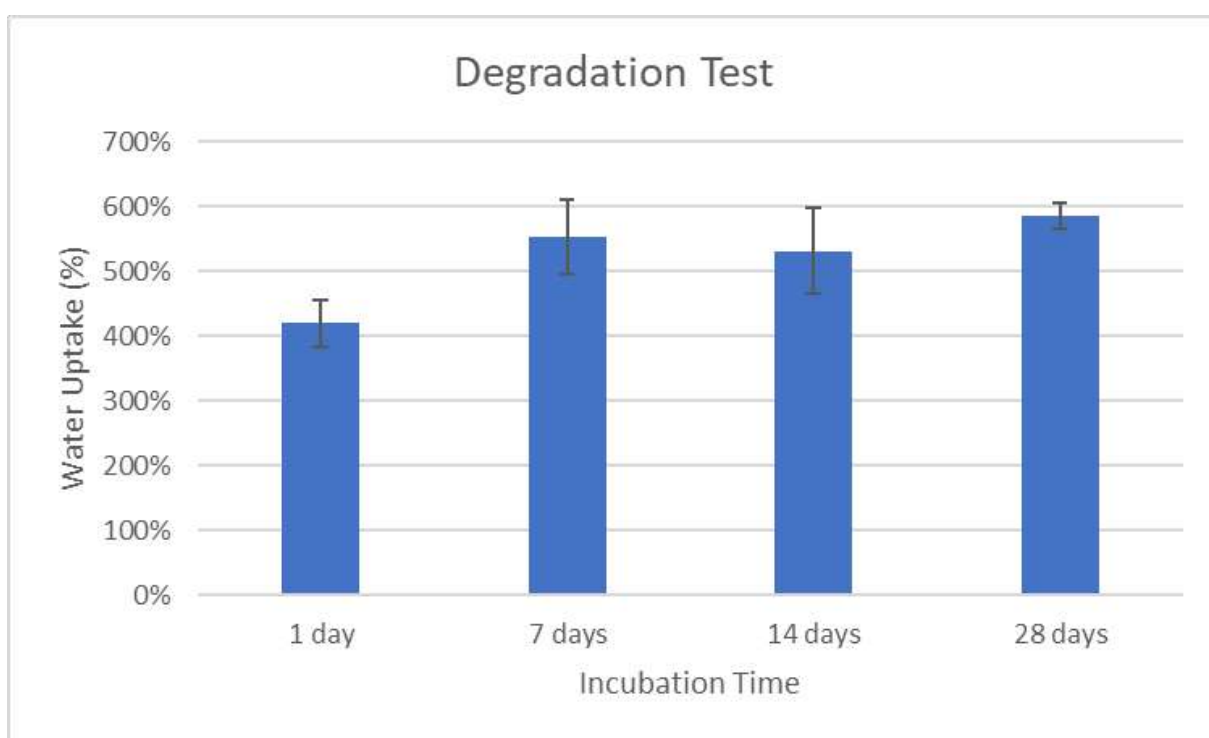


Figure 44: *Water Uptake vs Incubation Time for PCL/ZEIN 2:1 Random*

In this case, we can observe the exceptionally high values of water uptake despite PCL being hydrophobic. This could be attributed to the high porosity, as this capacity is directly related to the sample's surface area and diffusion within it.

On the other hand, the results of mass loss versus incubation time were analyzed, as shown in Figure 45. Here, it can be observed that the mass loss is almost negligible, and there is even a significant dispersion in the data that appears to indicate an increase in mass.

As seen in the SEM images, the structure of PCL/ZEIN remains almost intact over the days, as PCL reportedly takes months to degrade in vitro. The small dots observed could be attributed to ZEIN, and these may contribute to the minor mass loss values. The high dispersion in the values is due to errors in recording the mass of very small samples associated with handling and events of micro fragmentation.

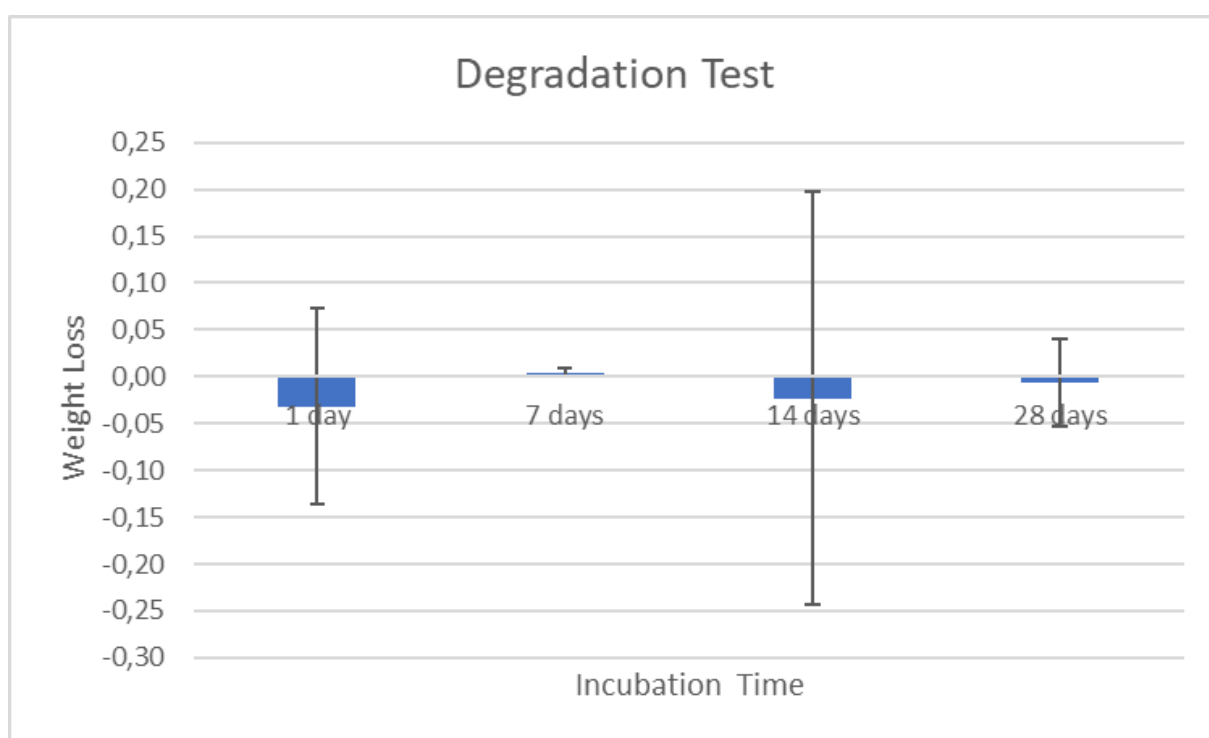


Figure 45: *Weight loss vs incubation time for PCL/ZEIN 2:1 (random)*

Speaking specifically about tendon regeneration, the fibers have to remain stable for the necessary time until the tissue can regenerate. The fact that there is no noticeable degradation at the end of this 28-day period is a good result since it shows that the fibers are resistant enough despite being blends of PCL and ZEIN. This is due to the presence of PCL, which is highly stable and in future research it will be necessary to study degradation for in vivo applications.

6.3 Cell Test

6.3.1 Cell Viability

The cell viability test is not a direct evaluation of the cells; rather, it aims to assess whether they grow and proliferate within our scaffolds or if they succumb to cell death due to potential toxicity of the scaffold. For this study, the PCL 20%, Zein CC (72 h), PCL/ZEIN 2:1 mats (random and aligned) were chosen. In addition we add medium without any cells and liquid only with cells as a reference.

We place the samples in the multiplate and on top we put cells with medium so that they proliferate as shown in figure 46. Cells take up the WST-8 molecule in the cytoplasm and metabolize it, using the mitochondrias to reduce it into smaller molecules that are expelled into the medium. If this happens over time, the color of the medium will change from red to orange and may even reach yellow. This is an indicator of how metabolically active the cells are, that is, if they develop correctly and how quickly they do so. In case the cells die you should not perceive any changes.



Figure 46: Plate used for cell viability and ALP Activity.

As can be seen in the Figure 47 left, after 7 days all the cells are capable of proliferating in our environment, being the zein-based scaffolds, the ones with a more orange coloration, giving the idea of a slightly faster proliferation. However, after 14 days (Figure 47 right) we can see that all the cells take on almost the same coloration, demonstrating that they allow their proliferation in the different selected scaffolds without any notorious difference.



Figure 47: Cell viability test. Left: After 7 days. Right: After 14 days.

Entering into data analysis, it is important to consider that the medium is not used as a target since the data may not reflect what is actually observed under the microscope. This arises from the conclusions of [27], so it is simply used as a control, for example, to verify the presence of contaminants.

Single cells serve as the positive control since they are cells that proliferate without any interference from a sample, and we consider this as 100%. Based on this, we compare the absorbance of all samples with respect to the single cells to obtain the results shown in Figure 48.

All the samples show a decrease in cell viability, this is expected because it is hard to maintain a culture in vitro on scaffolds over a long time. Compared to the well plate, cells have less space available, because scaffolds are providing a substrate for cell infiltration and growth. Also the nutrition is not optimal (exchanging the medium every 3-4 days is not the same as having a continuous exchange of nutrients as it is in the human body or with more complicated in vitro culture systems, like bioreactors). In this case zein sure can be used as it is a protein, but it's stable enough to remain there as part of the fibers.

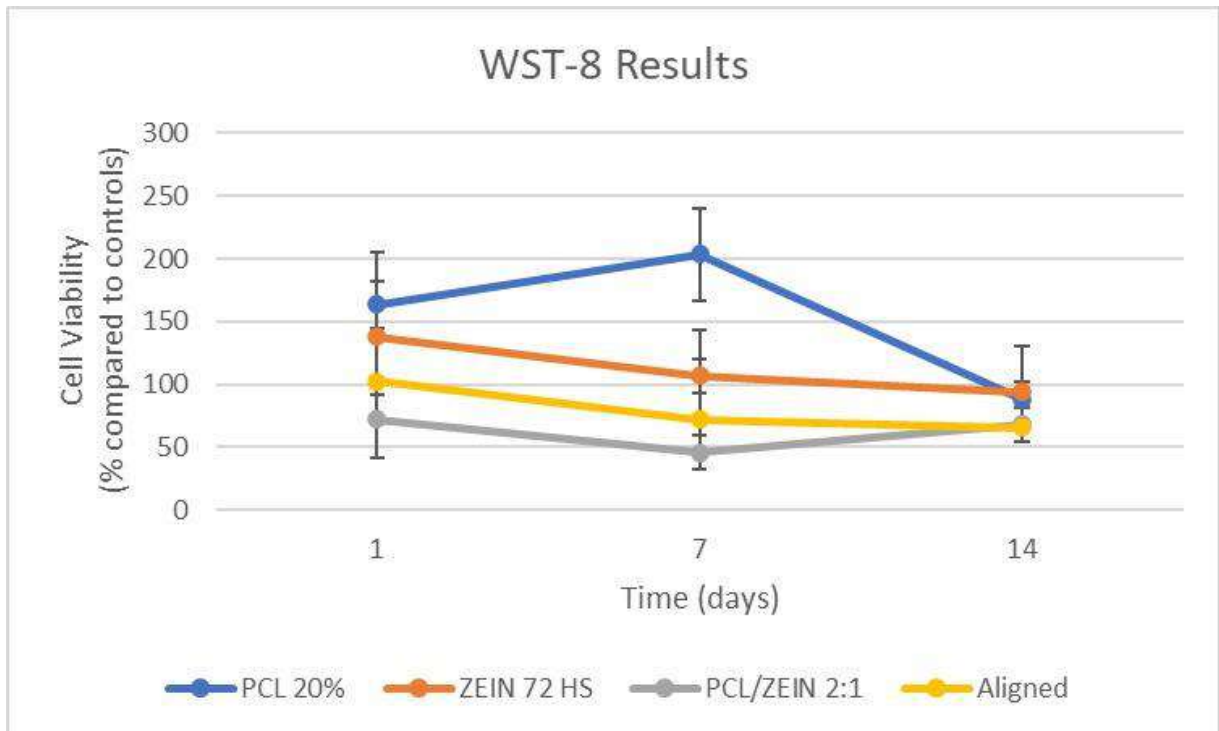


Figure 48: WST-8 Results

Figure 39 shows that cells are preferring the PCL 20%, at least until 7 days of culture. Maybe because of the topography of the fibers (optimal fiber diameter for cell attachment, optimal pore size for cell infiltration, while the aligned one maybe had too small pores for cells to penetrate, and only localized on the surface). Typically, cell adhesion assays are necessary to complement information.

As seen later, PCL/ZEIN blends appear to exhibit better cell adhesion behavior compared to PCL 20%, so one might expect better cell viability. However, this is not straightforward since with WST we are measuring mitochondrial activity, which is related to viability, but it is not an exact measurement. It could be that you have fewer cells on PCL, but they are stressed, which means they are more metabolically active.

Additionally, it's essential to note that every type of cell reacts uniquely when it comes into contact with a surface. The ability of cells to attach depends on various elements, including the specific cell type, the firmness of the surface, and how moist it is. As a result, it's plausible that the mechanical and physical properties of the material were not precisely calibrated to ensure an optimal bond between cells and the surface.

6.3.2 Cell Adhesion

We fixed the samples with the critical point dryer following the procedure explained in the methods. After that we saw them with the SEM to evaluate the morphology of the cells adhered to the materials investigated. This assay was conducted using PCL 20%, ZEIN CC 72 h, PCL/ZEIN 2:1 random, and aligned.

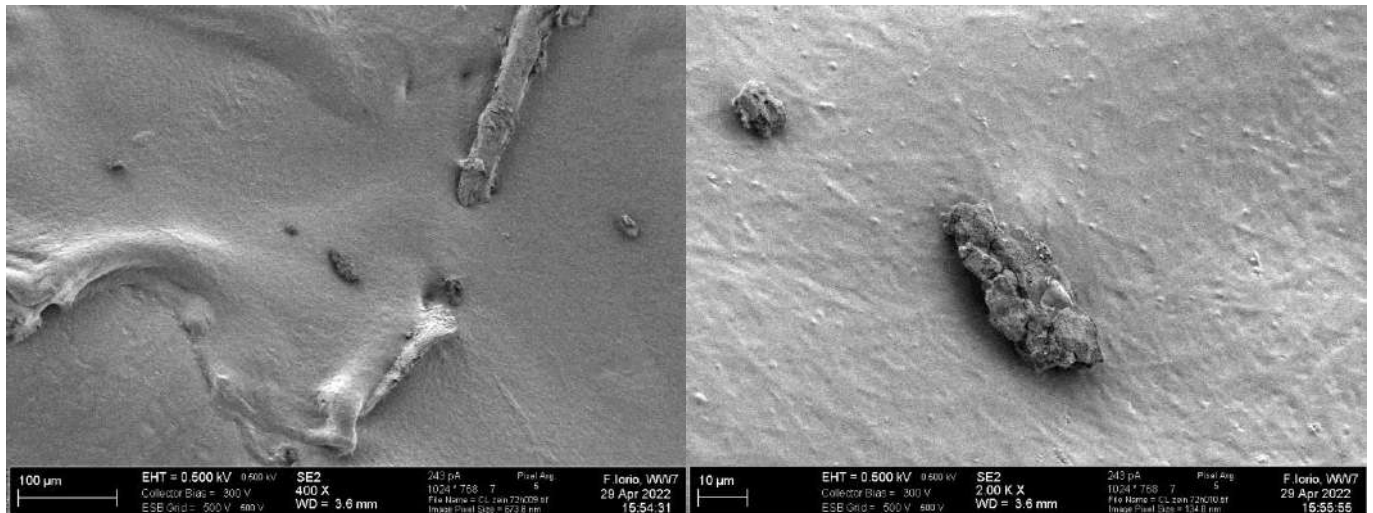


Figure 49: *Zein CC 72 h sample*

Starting with the analysis on the Zein CC 72 h, despite being crosslinked, it's not possible to observe any structure after 7 days of incubation with the medium in the WST-8 assay (Figure 49). This suggests that perhaps this number of days is too much for the material or perhaps the cells simply consumed the Zein. Thus, there are no longer any fibers, and we have a sort of melt/film.

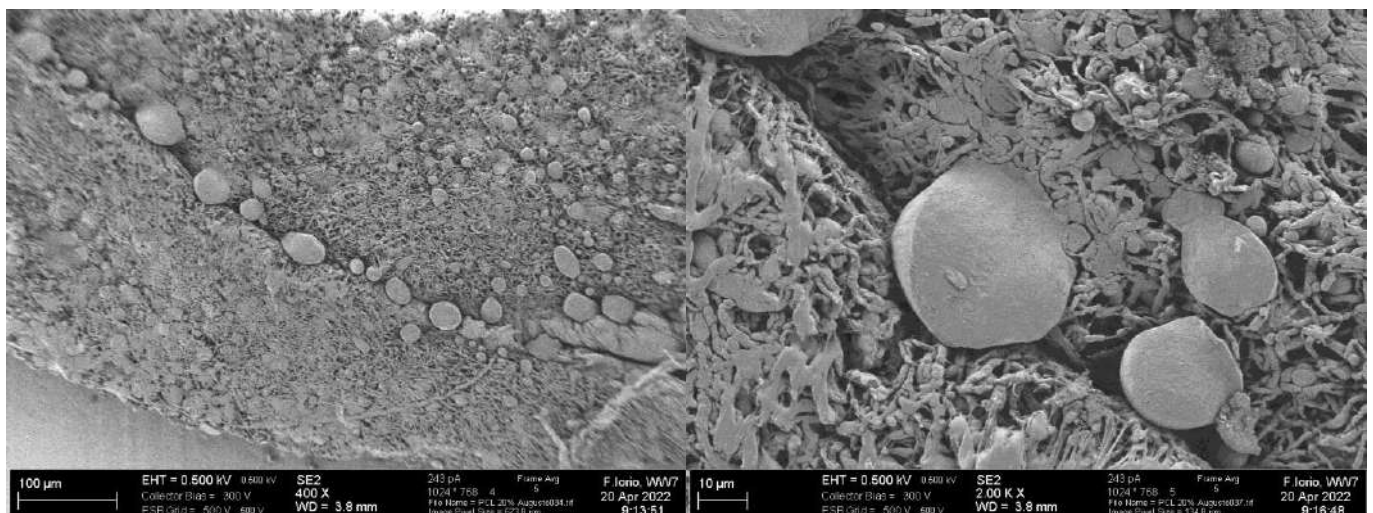


Figure 50: *PCL 20% Sample*

Continuing with the PCL 20% (Figure 50), unlike what was observed in the Zein, after the assays, the fibrous structure remains intact, and within it, some cells with a moderately spherical shape are visible. Although not very noticeable, with the presence of these cells under SEM, it can be confirmed that these cells are adhered. This is because otherwise, they would have washed away during the critical dried process.

Ideally, we would aim for these cells to be more elongated or spread on the surface, but perhaps 7 days is not enough for these samples. The scaffold may not be adapted for them to adhere, perhaps due to the stiffness not being right, among other reasons.

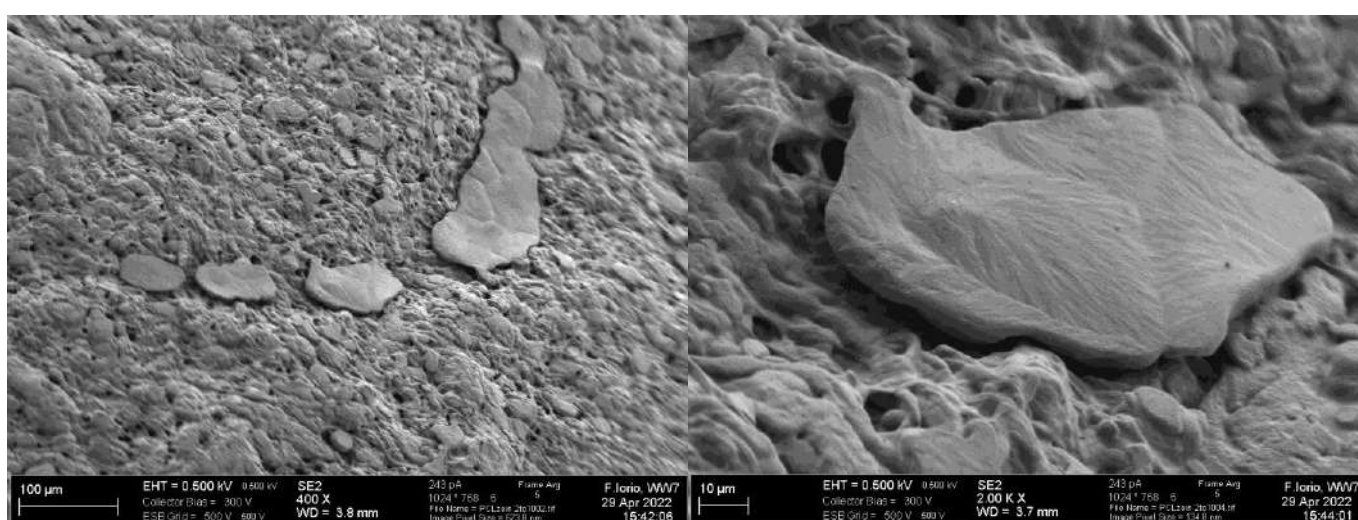


Figure 51: *PCL/ZEIN 2:1 random sample*

Analyzing the PCL/ZEIN random, we can see cells spread on the surface (they are not round), which is exactly the morphology we are looking for to ensure that the cells have a good adhesion to the matrix. These cells could have proliferated correctly and expanded on the surface of the sample.

However, if we compare it with what we see in figure 52, the cells in the aligned samples are a bit more rounded. This is not necessarily a bad result since they are adhered to the fibers, but perhaps 7 days is not enough for this new structure.

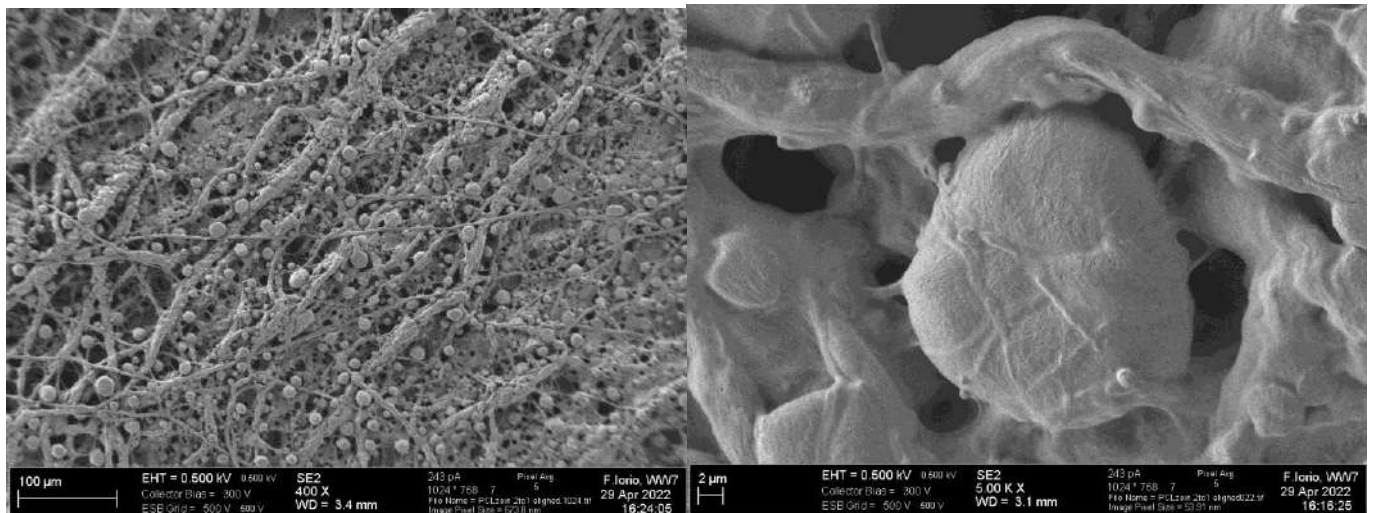


Figure 52: PCL/ZEIN 2:1 Aligned sample

In this test, we utilized fibroblasts because they closely resemble tenocytes and are expected to elongate. Several studies in the literature have shown satisfactory adhesion of fibroblasts to oriented structures; however, it is also demonstrated that they can be sensitive to topography [30]. In the case of the aligned fibers, we did not observe these results, which could be attributed to various reasons. It is possible that they were not sufficiently plastic due to their passage number being between 24 and 27, indicating older fibroblasts may have had difficulty adapting to stimuli and proliferating. This is because with each cell passage, they experience stress and age, becoming less metabolically active and requiring more time to duplicate DNA. It could be advantageous if these cells were tested at earlier passage numbers, ideally not too long after being taken directly from the body, as they would be more dynamic.

On the other hand, maybe the substrate did not possess the desired stiffness. However, it cannot be overlooked that despite their similarities, fibroblasts are not tenocytes. To better understand these results in future experiments, it would be beneficial to use tenocytes or stem cells instead. Perhaps they could adapt and attach better to the substrate and the aligned structure.

6.3.3 ALP Activity

The ALP protein is highly expressed in bone and when we speak about bone regeneration, the idea is to detect high ALP activity since I want my cells to behave like bone cells (osteoblast, osteoclast, etc).

However, since the focus is on tendon regeneration, the objective is slightly different. The tendon is mostly collagen, conferring certain key properties for its operation, such as mobility and elasticity, the opposite of the behavior of a bone, rigid and usually with very low elasticity. Although the idea of this assay is to verify that we have low or no cells that behave like bone cells to guarantee the behavior of the scaffold correctly. On the other hand maybe some areas may have slight ALP activity because the scaffold can also be used in a region close to the bone and we want it to be compatible with it.

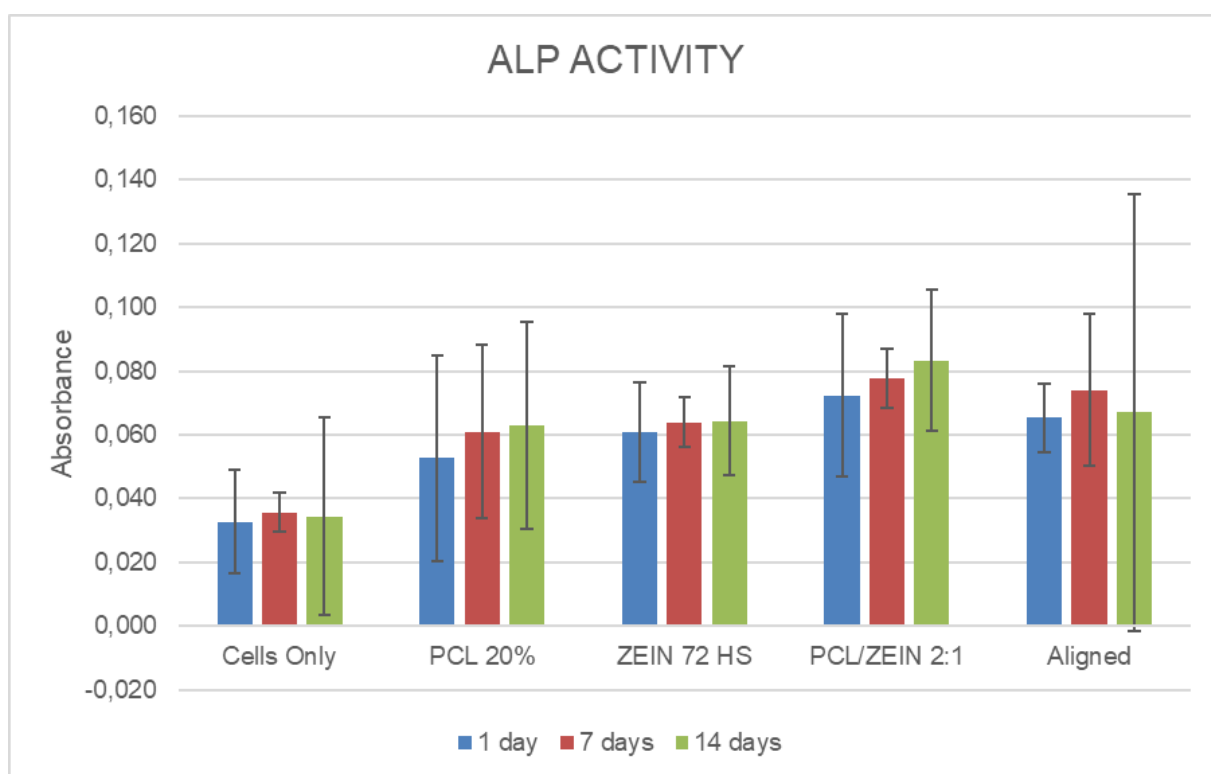


Figure 53: ALP activity vs incubation time

As I can't state that the ALP activity is an absolute value because it doesn't mean anything without the cells to compare them with another value. This value is the cells without scaffold to ensure that the same cells without scaffold showed some value of ALP activity. This is not high value because they are fibroblasts and should not differentiate into bone cells (osteoblasts/osteoclasts).

As we can see in Figure 53, there is a slight difference in the presence of the scaffold compared to the cells alone; however, it is not high enough to be considered significant. The results are what we expected because the tendon is flexible and must adapt to mechanical loads and should not be stiff. However, since the tendon inserts into the bone, it is expected that this part will have a more intermediate behavior and perhaps the amount of ALP will increase.

.

7. Conclusions

Eight types of scaffolds with various compositions were prepared using the electrospinning technique. In order to optimize this process, parameters such as voltage, flow rate, solvent, needle distance, spinning time, concentration, solvent, temperature or humidity. Through the optimization of these parameters, it was possible to produce electrospun PCL/ZEIN 2:1 aligned-based scaffolds.

Green solvents were successfully used to avoid toxic solvents, which are highly harmful for both the operator and the environment; moreover, residual traces of these solvents can compromise cell viability. Even for the crosslinking of zein, non-toxic solvents were employed to align with the project's objectives.

Regarding cell characterization, SEM analysis confirmed that the majority of samples exhibited defect-free structures, except for zein AA, which appeared to have dots and uneven fibers. All zein CC samples displayed a flat fiber structure with no noticeable difference between preparation times prior to electrospinning. PCL 20% displayed a bimodal structure, whereas the PCL/zein blend at a ratio of 2:1 showed the best results with a uniform and rounded fiber structure. Finally, PCL/zein blends at ratios of 1:1 and 1:2 exhibited more flattened fibers.

Based on these results and the resistance exhibited by the fibers to manipulation, it was decided to produce aligned fibers using the PCL/zein blend at a ratio of 2:1, resulting in bead-free mats. Furthermore, it was possible to measure direct

Additionally, under SEM analysis, the samples of PCL/ZEIN 2:1 showed no degradation of their structure beyond some dots attributed to zein zones. This suggests that the outer parts of the fibers contain a higher amount of zein, while the interior is composed of PCL. Indications of this can also be obtained through contact angle tests, degradation assays, and water uptake measurements.

FTIR spectra were conducted on all samples to confirm the presence of all functional groups of PCL and ZEIN in the different scaffolds. Ideally, FTIR would be performed also after degradation tests, but due to time constraints, this was not possible. However, based on observations, it would be expected that peaks associated with PCL remain unchanged while those related to zein decrease.

Through contact angle tests, it was confirmed that all PCL/ZEIN blends exhibit high permeability, as water drops completely penetrate the structure within 10 seconds or less. Additionally, one could infer that zein coats the PCL, giving it his hydrophilic character, and it favors tissue integration and cell functions.

Degradation tests confirmed the resilience of the PCL/ZEIN 2:1 blend, consistent with comparable data found in the literature. In vitro, PCL typically takes months to degrade, indicating that blending it with zein does not notably affect its degradation rate. Moreover, despite PCL being highly hydrophobic, its water uptake was found to be very high. This phenomenon may be attributed to the material's high porosity, which is directly linked to the surface area of the sample and the diffusion within it. Additionally, the presence of ZEIN could potentially coat the PCL, contributing to its hydrophobic behavior.

In the mechanical tests, separate evaluations were conducted on PCL and Zein to establish a baseline for their properties. Given that PCL demonstrates favorable mechanical properties whereas Zein does not, the aim was to assess the properties of their blends. However, crosslinked Zein displayed no enhancement; the samples proved excessively brittle even during handling for testing. Concerning the PCL/ZEIN blends, the 2:1 ratio exhibited superior characteristics compared to the other two ratios. Furthermore, the results of the aligned fibers, intended for tendon tissue engineering, were satisfactory, approaching the desired properties of tendon tissue.

Biological tests allowed us to investigate the proliferation capacity of cells within our scaffolds. The outcomes were promising, as cell adhesion was observed in nearly all samples studied, along with positive cell viability data. However, there were discrepancies among them regarding which samples cells exhibited a preference for, which could be attributed to various factors. Furthermore, ALP assays were conducted to confirm that the cells did not undergo differentiation into hard tissues such as bone. The findings were encouraging, as very low absorbance levels were recorded, indicating a likelihood of soft tissue formation. Nevertheless, within the specific context of tendon, some ALP activity might be anticipated, given that tendons insert into bone at their ends, suggesting a more intermediate behavior should be considered.

8. Future work

Assuming that the processing conditions were optimized for the PCL/ZEIN 2:1 blends, it would be ideal to repeat some measurements to minimize dispersion and deviation in the results. Moving into the characterization of the scaffolds, determining the size and distribution of the pores will be crucial for further analysis. The size and shape of the pores influence the mechanical and functional properties of the scaffolds, playing a completely influential role in tissue regeneration.

Mechanical tests should be conducted at least ten times to obtain a reliable value, in addition to adding measurements post-degradation. This should be done at various time intervals to gain a more realistic performance understanding of the samples over time. In relation to this, it would be ideal to analyze longer degradation periods, as the degradation times for these blends can span several months. Future research is necessary to examine how degradation would occur in vivo.

Delving into the details of the cell tests, it would be of vital importance to try working with tenocytes or stem cells. This could lead to a better understanding of these results in future experiments, as these cells might adapt and attach more effectively to the substrate and the aligned structure.

8. References

- 1) Maria Rita Citeroni, Maria Camilla Ciardulli, Valentina Russo, Giovanna Della Porta, Annunziata Mauro, Mohammad El Khatib, Miriam Di Mattia, Devis Galesso, Carlo Barbera, Nicholas R. Forsyth, Nicola Maffulli and Barbara Barboni. "In Vitro Innovation of Tendon Tissue Engineering Strategies". International journal of molecular sciences, September 2020
- 2) Kannus P. "Structure of the tendon connective tissue". Scandinavian Journal of Medicine and Science in Sports, 26 July 2000.
- 3) Chavaunne T. Thorpe and Hazel R.C. Screen. "Tendon Structure and Composition". Springer International Publishing Switzerland 2016.
- 4) Thorpe CT, Clegg PD, Birch HL "A review of tendon injury: why is the equine superficial digital flexor tendon most at risk?" Equine Vet, 2010.
- 5) Mike Bundy, Andy Leaver. "Guide to Sports and Injury Management". Churchill Livingstone, 2011
- 6) Boris A. Zelle, Freddie H. Fu "Rehabilitation for the Postsurgical Orthopedic Patient". Elsevier Inc, January 2013
- 7) Sensini A, Cristofolini L. "Biofabrication of Electrospun Scaffolds for the Regeneration of Tendons and Ligaments". Materials (Basel). 12 October 2018
- 8) Maria Rita Citeroni, Maria Camilla Ciardulli, Valentina Russo, Giovanna Della Porta, Annunziata Mauro, Mohammad El Khatib, Miriam Di Mattia, Devis Galesso, Carlo Barbera, Nicholas R. Forsyth, Nicola Maffulli and Barbara Barboni, "In vitro and in vivo assessments of an optimal polyblend composition of polycaprolactone/gelatin nanofibrous scaffolds for Achilles tendon tissue engineering" Journal of Industrial and Engineering Chemistry, 25 August 2019,
- 9) Wynn TA. "Fibrotic disease and the T(H)1/T(H)2 paradigm" Nat Rev Immunol. August 2004
- 10) Pierre-Olivier Bagnaninchi, Ying Yang, Alicia J El Haj, Nicola Maffulli, "Tissue engineering for tendon repair" Br J Sports Med. August 2007
- 11) Ruiz-Alonso S, Lafuente-Merchan M, Ciriza J, Saenz-Del-Burgo L, Pedraz JL. "Tendon tissue engineering: Cells, growth factors, scaffolds and production techniques" J Control Release. 10 May 2021
- 12) Carlos Joaquín Pérez-Guzmán and Roberto Castro-Muñoz. "A Review of Zein as a Potential Biopolymer for Tissue Engineering and Nanotechnological" Processes, 29 October 2020
- 13) A.M.S. Plath, S.P. Facchi, P.R. Souza, R.M. Sabino, E. Corradini, E.C. Muniz, K.C. Popat, L.C. Filho, M.J. Kipper, A.F. Martins. "Zein supports scaffolding capacity toward mammalian cells and bactericidal and antiadhesive properties on poly(ϵ -caprolactone)/zein electrospun fibers" Materials Today Chemistry June 2021
- 14) MOLFINO, H. Mauricio Gonzales; ALCALDE-YANEZ, Alexander; VALVERDE-MORON, Valery y VILLANUEVA-SALVATIERRA, Dulce. "Electrospinning: Avances y aplicaciones en el campo de la biomedicina". Rev. Fac. Med. Hum. 2020

- 15) Lina Marcela Duque Sánchez, Leonardo Rodríguez, Marcos López “ELECTROSPINNING: LA ERA DE LAS NANOFIBRAS” Revista Iberoamericana de Polímeros, November 2012
- 16) Vogt L, Liverani L, Roether JA, Boccaccini AR. “Electrospun Zein Fibers Incorporating Poly(glycerol sebacate) for Soft Tissue Engineering”. *Nanomaterials* (Basel). 2018
- 17) Y. Li, Q. Xia, K. Shi, “Scaling behaviors of zein in acetic acid solutions”, *J. Phys. Chem. B.* 2011
- 18) Wang H., Di L., Ren Q., Wang J. “Applications and degradation of proteins used as tissue engineering materials “. *Materials* 2009
- 19) L. Liverani, L. Vester, A.R. Boccaccini, “Biomaterials Produced via Green Electrospinning” Springer, *Electrospun Biomaterials and Related Technologies* 2017
- 20) ICH Harmonised Guideline “Impurities: guideline for residual solvents Q3C (R6)” ICH Expert Working Group 2016.
- 21) AGUSTINA MASSONE, “FABRICATION AND CHARACTERIZATION OF ELECTROSPUN ZEIN-BASED SCAFFOLDS FOR SOFT TISSUE ENGINEERING” - Universidad Nacional de Mar del Plata- Facultad de Ingeniería Friedrich-Alexander Universität Erlangen-Nürnberg 2017
- 22) Dippold D., Tallawi M., Tansaz S., Roether J. A., Boccaccini A. R. “Novel electrospun poly (glycerol sebacate)-zein fiber mats as candidate materials for cardiac tissue engineering”. *European Polymer Journal*, 2016.
- 23) Li Y., Lim L.-T., Kakuda Y. “Electrospun zein fibers as carriers to stabilize (-)- epigallocatechin gallate”. *Journal of food science*, 2009,
- 24) Corradini E., Mattoso L.H.C., Guedes C.G.F., Rosa D.S. “Mechanical, thermal and morphological properties of poly(ϵ -caprolactone)/zein blends”. *Polymers for advanced technologies*, 2004,
- 25) A. Doustgani¹ , E. Vasheghani-Farahani^{1*}, M. Soleimani² , S. Hashemi-Najafabadi. “Preparation and Characterization of Aligned and Random Nanofibrous Nanocomposite Scaffolds of Poly (Vinyl Alcohol), Poly (e-Caprolactone) and Nanohydroxyapatite“. *Tarbiat Modares University*, 2011
- 26) Fabrication and properties of porous scaffold of zein/PCL biocomposite for bone tissue engineering Fan Wu a , Jie Wei b , Changsheng Liu b , Brian O'Neill a , Yung Ngothai a,† East China University of Science and Technology, Shanghai 200237, China
- 27) Francesco Iorio, “Polysaccharide-coated electrospun matrices for wound dressing: an in vitro study on keratinocytes”. *TESI SPERIMENTALE UNIVERSITÀ DEGLI STUDI DI TRIESTE* 2019
- 28) Marta Ibañez Martín, “Biomecánica del músculo y el tendón. Análisis crítico de modelos teórico-numéricos”. *Universidad Politécnica de Madrid*, Febrero 2022
- 29) Lina Chen, Casey Yan, Zijian Zheng “Functional polymer surfaces for controlling cell behaviors” *The Hong Kong Polytechnic University, Hung Hom, Kowloon* 2018
- 30) Deok-Ho Kim, Karam Han, Kshitiz Gupta, Keon Woo Kwon, Kahp-Yang Suh and Andre Levchenko, “Mechanosensitivity of fibroblast cell shape and movement to anisotropic substratum topography gradients”. *Biomaterials*. 30 October 2009